Bmix

**NASA TECHNICAL NOTE**

**NASA TN D-7363**

NASA TN D-7363



# FIXED-BASE SIMULATION STUDY OF DECOUPLED CONTROLS DURING APPROACH AND LANDING OF A STOL TRANSPORT AIRPLANE

*by G. Kimball Miller, Jr., Perry L. Deal, and Robert A. Champine*

*Langley Research Center*
*Hampton, Va. 23665*

NATIONAL AERONAUTICS AND SPACE ADMINISTRATION • WASHINGTON, D. C. • FEBRUARY 1974

| 1. Report No. | 2. Government Accession No. | 3. Recipient's Catalog No. |
|---|---|---|
| NASA TN D-7363 | | |
| 4. Title and Subtitle<br>FIXED-BASE SIMULATION STUDY OF DECOUPLED CONTROLS DURING APPROACH AND LANDING OF A STOL TRANSPORT AIRPLANE | | 5. Report Date<br>February 1974<br>6. Performing Organization Code |
| 7. Author(s)<br>G. Kimball Miller, Jr., Perry L. Deal, and Robert A. Champine | | 8. Performing Organization Report No.<br>L-8825 |
| 9. Performing Organization Name and Address<br>NASA Langley Research Center<br>Hampton, Va. 23665 | | 10. Work Unit No.<br>501-26-05-03<br>11. Contract or Grant No. |
| 12. Sponsoring Agency Name and Address<br>National Aeronautics and Space Administration<br>Washington, D.C. 20546 | | 13. Type of Report and Period Covered<br>Technical Note<br>14. Sponsoring Agency Code |
| 15. Supplementary Notes | | |

16. Abstract

A fixed-base visual simulation study has been conducted to evaluate the use of decoupled controls as a means for reducing pilot workload during approach and landing of an externally blown jet-flap short take-off and landing (STOL) transport. All six rigid-body degrees of freedom were employed with the aerodynamic characteristics based on wind-tunnel data. The primary piloting task was to use a flight director to capture and maintain a two-segment glide slope, with a closed-circuit television display of a STOL airport used during simulations of the flare and landing. The decoupled longitudinal controls used constant prefilter and feedback gains to provide steady-state decoupling of flight-path angle, pitch angle, and forward velocity. The pilots were enthusiastic about the decoupled longitudinal controls but believed the decoupled concept offered no significant advantage over conventional controls in the lateral mode.

| 17. Key Words (Suggested by Author(s)) | 18. Distribution Statement |
|---|---|
| STOL handling qualities<br>Decoupled control systems<br>Terminal area control | Unclassified – Unlimited<br><br>STAR Category 02 |

| 19. Security Classif. (of this report) | 20. Security Classif. (of this page) | 21. No. of Pages | 22. Price* |
|---|---|---|---|
| Unclassified | Unclassified | 62 | $3.50 |

*For sale by the National Technical Information Service, Springfield, Virginia 22151

# FIXED-BASE SIMULATION STUDY OF DECOUPLED CONTROLS DURING APPROACH AND LANDING OF A STOL TRANSPORT AIRPLANE

By G. Kimball Miller, Jr., Perry L. Deal,
and Robert A. Champine
Langley Research Center

## SUMMARY

A fixed-base visual simulation study has been conducted to evaluate the use of decoupled controls as a means for reducing pilot workload during approach and landing of an externally blown jet-flap short take-off and landing (STOL) transport. All six rigid-body degrees of freedom were employed, with the aerodynamic characteristics based on measured wind-tunnel data. The primary piloting task was to use a flight director to capture and maintain a two-segment glide slope, with a closed-circuit television display of a STOL airport used during simulations of the flare and landing.

The decoupled longitudinal controls employed constant prefilter and feedback gains to provide steady-state decoupling of flight-path angle, pitch angle, and forward velocity and thus avoided the necessity of an onboard computer. The pilots stated they could obtain the desired glide slope more easily and with less workload using decoupled longitudinal controls than with conventional controls, as indicated by an improvement in pilot rating of one-half increment. The pilot ratings for the flare-to-landing maneuver were improved from 3 to 2 by using decoupled longitudinal controls, primarily because of the precision with which the flight-path angle could be controlled in ground effects. These pilot ratings are for a two-segment approach with the second glide slope equal to $4^{\circ}$. The pilot ratings degrade as the second angle is steepened but are unaffected by changes in the initial glide slope from $6^{\circ}$ to $9^{\circ}$. When the decoupled longitudinal controls were employed in performing decelerating approaches from approximately 120 to 70 knots, they were given a pilot rating of 3 or better.

When decoupled lateral controls were implemented to provide independent control of yaw rate and sideslip angle, the result was given a pilot rating of 2, primarily because of reduced response to turbulence. The pilots believed, however, that the decoupled control concept offered no significant advantage over conventional controls with stability augmentation system (SAS) in the lateral mode.

## INTRODUCTION

There is currently considerable interest in short take-off and landing (STOL) transport aircraft as a means for alleviating air-traffic congestion that is increasing in most metropolitan areas. In order to retain efficient cruise characteristics STOL aircraft must have high wing loadings. Consequently, the low approach and landing speeds necessary for landing on 610-meter (2000-ft) runways require the production of high lift coefficients. One method of obtaining high lift coefficients is through the use of externally blown jet flaps to provide powered lift by deflecting the jet exhaust (see refs. 1, 2, and 3). The operational requirements of STOL aircraft necessitate very precise control capability; however, their handling qualities are poor compared with conventional aircraft. The unaugmented jet-flap STOL airplane in an early simulation study (ref. 4) was rated unsatisfactory longitudinally and unacceptable laterally. Conventional stability augmentation systems (SAS) have been applied (refs. 4 and 5) to the jet-flap STOL aircraft to obtain satisfactory handling qualities for the approach and landing task.

The present simulation study employs decoupled controls rather than conventional SAS in an attempt to reduce the high pilot workload situation that exists during approach and landing. During the initial phase of the study decoupled control of the longitudinal mode is employed (the movement of the horizontal tail, flaps, symmetric spoilers, and throttle are automatically controlled so as to provide independent or decoupled control of pitch angle, flight-path angle, and forward velocity) while the conventional SAS of reference 5 is retained for the lateral mode. During the later phases of the study the decoupled-controls concept was incorporated in the lateral mode. The decoupled lateral controls employed the spoilers, rudder, and ailerons to provide independent control of yaw rate and sideslip angle. It should be emphasized that the decoupled controllers being studied in this investigation require no onboard computations and can be easily added to an airplane as a set of constant gains.

In order to compare decoupled controls with stability augmentation of conventional controls, the current investigation employed the same simulation program as reference 5, including the same research pilots. The simulation employed real-time digital computation of the six-degree-of-freedom nonlinear equations of motion representing the STOL airplane defined by the aerodynamic data presented in references 1, 2, and 3. The study used a fixed-base cockpit with a visual display of a STOL airport generated by closed-circuit television. The simulation included the effects of turbulence, crosswinds, and ground effects during the landing approach.

## SYMBOLS

Calculations for the investigation were made in U.S. Customary Units but are also given in the International System of Units (SI).

$A$ matrix of aircraft stability derivatives

$a_X, a_Y, a_Z$ longitudinal, lateral, and normal acceleration, respectively, g units

$B$ matrix of aircraft-control coefficients

$b$ wing span, meters (ft)

$C$ matrix relating desired output vector to state vector

$C_L$ lift coefficient

$C_l$ rolling-moment coefficient

$C_m$ pitching-moment coefficient

$C_n$ yawing-moment coefficient

$C_T$ thrust coefficient

$C_W$ aircraft weight in coefficient form $\left(-\frac{2mg}{\rho V^2 S}\right)$

$C_X$ longitudinal-force coefficient

$C_Y$ side-force coefficient

$C_Z$ normal-force coefficient

$c$ mean aerodynamic chord, meters (ft)

$e_i$ ith iteration of general variable $e$

| | |
|---|---|
| $F$ | matrix of feedback gains used in decoupled controller (see appendix A) |
| $G$ | matrix of prefilter gains used in decoupled controller (see appendix A) |
| $g$ | acceleration due to gravity, meters/second$^2$ (ft/sec$^2$) |
| $h$ | altitude, meters (ft) |
| $I$ | identity matrix |
| $I_X,I_Y,I_Z$ | moments of inertia about X, Y, and Z body axes, respectively, kilogram-meters$^2$ (slug-ft$^2$) |
| $I_{XZ}$ | product of inertia, kilogram-meters$^2$ (slug-ft$^2$) |
| $J$ | performance index used in determining optimal control (see appendix A) |
| $K$ | gain |
| $m$ | mass of airplane, kilograms (slugs) |
| $n$ | number of flights |
| $P$ | solution to matrix Riccati equation (see appendix A) |
| $P_{ph}$ | period of phugoid mode, seconds |
| $P_R$ | period of roll mode, seconds |
| $P_{sp}$ | period of short-period mode, seconds |
| $p,q,r$ | angular velocities about X, Y, and Z body axes, respectively, degrees/second or radians/second |

| | |
|---|---|
| $Q$ | state variable weighting matrix used in performance index $J$ |
| $R$ | control variable weighting matrix used in performance index $J$ |
| $R_a$ | range, measured on Earth's surface, from aircraft to landing-approach beacon, meters (ft) |
| $\bar{r}$ | vector of commanded inputs by pilot |
| $S$ | wing area, meters$^2$ (ft$^2$) |
| $s$ | Laplace operator |
| $T$ | total thrust, newtons (lbf) |
| $t$ | time, seconds |
| $\left(t_{1/2}\right)_{ph}$ | time to damp phugoid to one-half amplitude, seconds |
| $\left(t_{1/2}\right)_{R}$ | time to damp roll mode to one-half amplitude, seconds |
| $\left(t_{1/2}\right)_{sp}$ | time to damp short-period mode to one-half amplitude, seconds |
| $u,v,w$ | velocity components along $X$, $Y$, and $Z$ body axes, respectively, meters/second (ft/sec) |
| $\bar{u}$ | vector of control variables |
| $\hat{u}$ | difference between instantaneous control vector and vector of pilot inputs |
| $V$ | airspeed, knots (ft/sec) |
| $x,y,z$ | inertial axes located at runway threshold with positive $x$ down runway and positive $y$ to right |
| $\bar{x}$ | vector of state variables |
| $\bar{x}_e$ | vector of state variables at equilibrium conditions |
| $\hat{x}$ | difference between instantaneous and equilibrium state vectors |

$\bar{y}$ vector of state variables to be controlled in a decoupled manner

$Z_{lg}$ distance of landing gear from airplane center of gravity along Z body axis, meters (ft)

$\alpha$ angle of attack, degrees

$\beta$ angle of sideslip, degrees

$\gamma$ flight-path angle, degrees

$\delta_a$ aileron deflection, positive for right roll, degrees or radians

$\delta_{f1},\delta_{f2},\delta_{f3}$ deflection of forward, middle, and rearward segment of trailing-edge flaps (see fig. 2), degrees or radians

$\delta_{\overline{f3}}$ $\delta_{f3} - 60^{\circ}$, degrees

$\delta_{LT}$ cockpit controller for longitudinal trim

$\delta_r$ rudder deflection, degrees or radians

$\delta_s$ asymmetric deflection of spoilers, positive for right roll, degrees or radians

$\delta_{sp}$ symmetric spoiler deflection, degrees or radians

$\delta_t$ horizontal-tail deflection, degrees or radians

$\delta_{th}$ throttle deflection

$\delta_w$ wheel deflection, degrees or radians

$\epsilon_y$ localizer error, degrees

$\epsilon_z$ glide-slope error, $\tan^{-1}\left(\frac{h - Z_{lg}}{R_a}\right) - \theta_{gs}$, degrees

$\zeta_{ph}$ phugoid damping ratio

$\zeta_R$ roll-mode damping ratio

$\zeta_{sp}$ short-period damping ratio

$\theta_{gs}$ glide slope of landing-approach beacon, degrees

$\mu$ arithmetic mean, $\dfrac{\sum_{i=1}^{n} e_i}{n}$

$\rho$ air density, kilograms/meter$^3$ (slugs/ft$^3$)

$\sigma$ standard deviation, $\left[\dfrac{\sum_{i=1}^{n} \left(e_i - \mu\right)^2}{n - 1}\right]^{1/2}$

$\psi,\theta,\phi$ Euler angles of rotation relating body and inertial axes, referred to as yaw, pitch, and roll, respectively, degrees or radians

$\omega_{ph}$ phugoid natural frequency, radians/second

$\omega_R$ rolling natural frequency, radians/second

$\omega_{sp}$ longitudinal short-period natural frequency, radians/second

Aircraft stability and control coefficients:

$C_{l_\beta} = \dfrac{\partial C_l}{\partial \beta}$ $C_{n_\beta} = \dfrac{\partial C_n}{\partial \beta}$ $C_{Y_\beta} = \dfrac{\partial C_Y}{\partial \beta}$

$C_{X_{\delta_{\overline{f3}}}} = \dfrac{\partial C_X}{\partial \delta_{\overline{f3}}}$ $C_{Z_{\delta_{\overline{f3}}}} = \dfrac{\partial C_Z}{\partial \delta_{\overline{f3}}}$ $C_{m_{\delta_{\overline{f3}}}} = \dfrac{\partial C_m}{\partial \delta_{\overline{f3}}}$

$C_{X_{\delta_s}} = \dfrac{\partial C_X}{\partial \delta_s}$ $C_{Z_{\delta_s}} = \dfrac{\partial C_Z}{\partial \delta_s}$ $C_{m_{\delta_s}} = \dfrac{\partial C_m}{\partial \delta_s}$

$$C_{l_{\delta_s}} = \frac{\partial C_l}{\partial \delta_s} \qquad C_{n_{\delta_s}} = \frac{\partial C_n}{\partial \delta_s} \qquad C_{Y_{\delta_s}} = \frac{\partial C_Y}{\partial \delta_s}$$

$$C_{X_{\delta_{sp}}} = \frac{\partial C_X}{\partial \delta_{sp}} \qquad C_{Z_{\delta_{sp}}} = \frac{\partial C_Z}{\partial \delta_{sp}} \qquad C_{m_{\delta_{sp}}} = \frac{\partial C_m}{\partial \delta_{sp}}$$

$$C_{X_{\delta_t}} = \frac{\partial C_X}{\partial \delta_t} \qquad C_{Z_{\delta_t}} = \frac{\partial C_Z}{\partial \delta_t} \qquad C_{m_{\delta_t}} = \frac{\partial C_m}{\partial \delta_t}$$

$$C_{l_{\delta_r}} = \frac{\partial C_l}{\partial \delta_r} \qquad C_{n_{\delta_r}} = \frac{\partial C_n}{\partial \delta_r} \qquad C_{Y_{\delta_r}} = \frac{\partial C_Y}{\partial \delta_r}$$

$$C_{l_{\delta_a}} = \frac{\partial C_l}{\partial \delta_a} \qquad C_{n_{\delta_a}} = \frac{\partial C_n}{\partial \delta_a} \qquad C_{Y_{\delta_a}} = \frac{\partial C_Y}{\partial \delta_a}$$

$$C_{l_p} = \frac{\partial C_l}{\partial \frac{pb}{2V}} \qquad C_{n_p} = \frac{\partial C_n}{\partial \frac{pb}{2V}} \qquad C_{Y_p} = \frac{\partial C_Y}{\partial \frac{pb}{2V}}$$

$$C_{l_r} = \frac{\partial C_l}{\partial \frac{rb}{2V}} \qquad C_{n_r} = \frac{\partial C_n}{\partial \frac{rb}{2V}} \qquad C_{Y_r} = \frac{\partial C_Y}{\partial \frac{rb}{2V}}$$

$$C_{X_u} = \frac{\partial C_X}{\partial \frac{u}{V}} \qquad C_{Z_u} = \frac{\partial C_Z}{\partial \frac{u}{V}} \qquad C_{m_u} = \frac{\partial C_m}{\partial \frac{u}{V}}$$

$$C_{X_\alpha} = \frac{\partial C_X}{\partial \alpha} \qquad C_{Z_\alpha} = \frac{\partial C_Z}{\partial \alpha} \qquad C_{m_\alpha} = \frac{\partial C_m}{\partial \alpha}$$

$$C_{X_q} = \frac{\partial C_X}{\partial \frac{qc}{2V}} \qquad C_{m_q} = \frac{\partial C_m}{\partial \frac{qc}{2V}}$$

$$C_{X_{\dot\alpha}} = \frac{\partial C_X}{\partial \frac{\dot\alpha c}{2V}} \qquad C_{m_{\dot\alpha}} = \frac{\partial C_m}{\partial \frac{\dot\alpha c}{2V}}$$

Superscripts:

| | |
|---|---|
| T | matrix transpose |
| -1 | matrix inverse |
| ' | nondimensional perturbations from equilibrium |

Subscripts:

| | |
|---|---|
| 0 | trim condition |
| c | commanded by pilot |
| ge | ground effects |
| $\dot{h}$ | sink rate |
| x | touchdown position relative to runway threshold |
| w | gust intensity |
| X,Y,Z | aircraft body axes |

Abbreviations:

| | |
|---|---|
| EBF | externally blown flap |
| IFR | instrument flight rules |
| PR | pilot rating |
| rms | root mean square |
| SAS | stability augmentation system |
| STOL | short take-off and landing |

A dot over a symbol denotes differentiation with respect to time.

## SIMULATED-AIRPLANE DESCRIPTION

The STOL airplane simulated in this study is the clustered-engine aircraft simulated in reference 5 and aerodynamically described in references 1, 2, and 3. The aircraft (fig. 1) is a high-wing jet transport with four high bypass ratio turbofan engines. The four engines yielded a maximum total thrust of 147 057 N (33 060 lbf). The engine response characteristics for the airplane are tabulated in table I.

For the approach and landing condition the wing leading-edge flaps were deflected $60^{\circ}$, and the full-span, triple-slotted trailing-edge flaps had three segments, $\delta_{f1}$, $\delta_{f2}$, and $\delta_{f3}$, set at $25^{\circ}$, $10^{\circ}$, and $60^{\circ}$, respectively (see fig. 2). In the present investigation only the rear flap element was varied for control. Flap deflection $\delta_{f3}$ is comprised of the deflection of all three spanwise flap elements shown in figure 1. In addition, the inboard elements could be deflected differentially as ailerons $\delta_a$. The inboard flap elements were used as ailerons because they are more effective (ref. 1) in providing rolling moments than the other flap elements. The physical characteristics of the simulated aircraft including maximum control-surface deflection and deflection rate are presented in table II. A time lag of 0.1 second was employed for all control surfaces to account for system delays. The aerodynamic characteristics are presented in table III.

## DECOUPLED CONTROL

The general approach taken in providing independent or decoupled control of pitch angle, flight-path angle, and forward velocity is depicted in the following sketch:

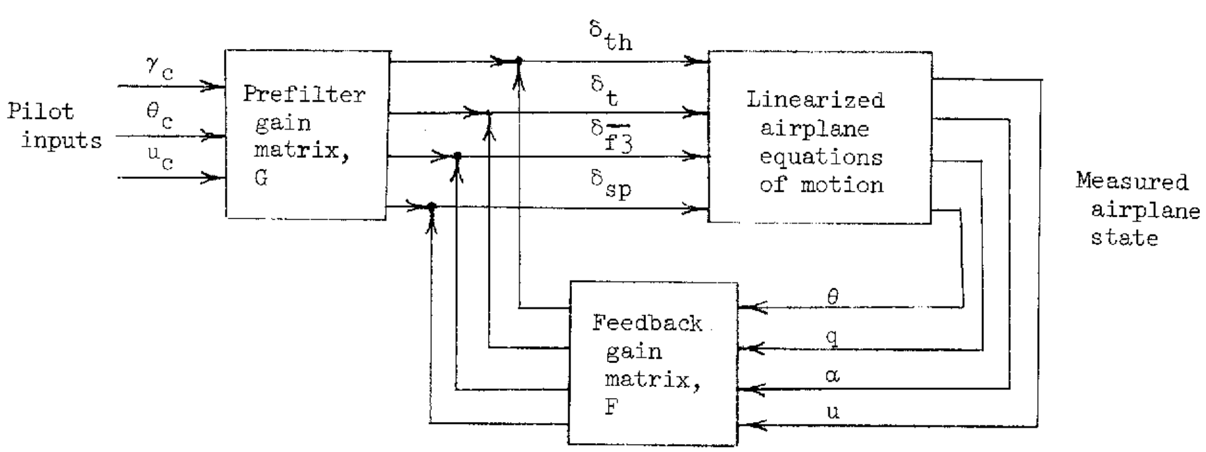


The decoupled controller was mechanized so that the pilot commanded flight-path angle $\gamma_c$ through inputs to the column, pitch angle $\theta_c$ through the flap lever, and forward velocity $u_c$ through the throttle. In addition, the thumb controller on the left horn of the control yoke was used to trim flight-path angle $\gamma$ so the pilot would not have to hold the column forward for a descent maneuver. The decoupled controller requires that the airplane pitch angle, pitch rate, angle of attack, and forward velocity be continuously measured. In this simulation study the measurements were assumed to be perfect.

The feedback gain matrix F and prefilter gain matrix G result in the aircraft control elements (throttle $\delta_{th}$, horizontal tail $\delta_t$, flaps $\delta_{\overline{f3}}$, and symmetric spoilers $\delta_{sp}$) moving so as to produce decoupled control of flight-path angle, pitch angle, and forward velocity as commanded by the pilot. There are a number of ways to obtain the feedback and prefilter gain matrices, F and G, required for decoupled longitudinal control. The most versatile method would be through the use of an onboard computer to find the time-varying adaptive gains. This high degree of sophistication may not be required if the decoupled controller is applied only to the approach and landing phase of operation and excludes other regimes. In this latter case, which was used in the present study, the gains F and G can be made constants, and thus the need for an onboard computer is avoided by requiring that the commanded aircraft states $\gamma_c$, $\theta_c$, and $u_c$ be decoupled only in the steady-state conditions. (See appendix A.) The development of the decoupled lateral controls is presented in appendix B.

## SIMULATION EQUIPMENT

The digital-computer program used in the present simulation employed nonlinear equations of motion for six rigid-body degrees of freedom. The turbulence model used in the study was based on the Dryden spectral form (ref. 5) having root-mean-square (rms) values up to 1.2 meters/second (4 ft/sec). The pilots felt that higher values were unrealistic. It is believed that the primary objection to the turbulence stemmed from the fixed-base nature of the simulation. The pilots stated that, in flight light to moderate turbulence was primarily felt rather than seen, whereas with the fixed-base simulator it was necessary to present the turbulence to the pilots through the aircraft instrumentation.

The fixed-base transport-type cockpit (fig. 3) was equipped with conventional flight and engine-thrust control devices. The simulator control forces were provided through a hydraulic servosystem as functions of control displacement and rate. The characteristics of the simulator control system are presented in table IV. The flight-instrument display was representative of current transport aircraft. Instruments indicating angle of attack, sideslip angle, and flap angle were included. The localizer channel of the conventional cross-pointer type flight director was driven as indicated in appendix A of reference 5. The glide-slope channel, however, was driven by the raw glide-slope error signal $\epsilon_z$ and did not include the incremental thrust signal used in reference 5 because the use of the decoupled longitudinal control system removes the necessity of the pilot manipulating thrust to control glide slope.

The visual cues for flare and landing were obtained by means of a 675-scan-line color television camera in conjunction with an optical pickup similar to that in reference 6. The optical pickup was driven by the output of the moment equations to provide the three rotational degrees of freedom of the aircraft. The three translational degrees of freedom were obtained by mounting the optical pickup and camera on a transport system that moved relative to a terrain model in response to the output of the force equations. The terrain model (fig. 4) was a three-dimensional $\frac{1}{300}$-scale model of the area around a STOL airport. The visual display was presented to the pilot through a television monitor and collimating lens system mounted in the pilot's windshield. Each flight was terminated at touchdown. The pilots could evaluate the characteristics of a series of decoupled systems quite rapidly because the simulation included a subprogram for computing the mathematically optimal gains for a specific set of weighting terms in the decoupled longitudinal controller. Consequently, the weighting terms on the aircraft state and control variables in the performance index (see appendix A) could be changed after each flight as functions of pilot opinion with the new optimal gains being computed within milliseconds.

## TEST PROGRAM

The pilot's task was to assume command of the aircraft in level flight and use the flight director to capture and maintain the localizer and glide slope under IFR conditions. The flights were initiated at an altitude of approximately 243.8 meters (800 ft) at varying distances from the runway (such that the airplane was initially below the glide slope) and with lateral offsets from the runway center line up to 61 meters (200 ft). At an altitude of 61 meters (200 ft) the pilot was to visually acquire the 914-meter (3000-ft) runway and land in a prescribed area. The pilots were instructed to land in the 137.2 meters (450 ft) long area marked on the runway (fig. 5) with sink rates of less than 1 meter/second (3 ft/sec). The basic restrictions on the airplane were the same as used in reference 5: the angle of attack for the approach conditions should be at least $10^{\circ}$ below the stall, and the approach speed should be at least 15 knots greater than the one-engine-out stall speed. The normal approach was performed at 70 knots using a two-segment approach in which a $6^{\circ}$ glide slope was followed to an altitude of 61 meters (200 ft) at which point transition was made to a $4^{\circ}$ glide slope. Selected flights were made in which the initial $6^{\circ}$ segment was maintained all the way to the flare just prior to touchdown, while other flights used initial segments as steep as $9^{\circ}$. Still other flights were performed in which the pilots were required to decelerate from approximately 120 knots to 70 knots while maintaining the glide slope. The flights were performed in turbulence with gusts having rms values between 0 and 1.2 meters/second (4 ft/sec). In addition, the adverse ground effects employed in reference 5 were again used. These ground effects cause a nose-down pitching moment and a decrease in lift and drag as the ground is approached.

## RESULTS AND DISCUSSION

The results of the investigation are divided into three major areas: constant-speed approaches using decoupled longitudinal controls, constant-speed approaches using decoupled longitudinal and lateral controls, and decelerating approaches using decoupled longitudinal and lateral controls. The major portion of the results will be in the form of pilot ratings (PR) using the rating system shown in table V. The pilot ratings presented herein reflect system performance both in and out of turbulence.

### Decoupled Longitudinal Controls

Although the general development of the decoupled longitudinal controller presented in appendix A included all four control elements – throttle, horizontal tail, flaps, and symmetric spoilers – only three are required to provide steady-state decoupling of the three state variables, flight-path angle, pitch angle, and forward velocity. One such mechanization used the throttle, the horizontal tail, and the flaps to provide decoupled control of flight-path angle, pitch angle, and forward velocity. The gains the pilots felt provided the best response are presented in table VI along with the resulting airplane stability characteristics.

The time history of a typical flight in turbulence with a rms gust intensity of 0.61 meter/second (2 ft/sec) is presented in figure 6 for a two-segment approach in which the desired glide-slope changes from $6^{\circ}$ to $4^{\circ}$ at an altitude of approximately 61 meters (200 ft) 42 seconds into the flight. This flight was initiated with the airplane in level flight 2 seconds prior to intersecting the $6^{\circ}$ glide-slope signal. The pilot was able to obtain the $6^{\circ}$ glide slope and keep the glide-slope error $\epsilon_z$ less than about half a degree until the beginning of flare approximately 10 seconds prior to touchdown and landed in the desired area with a sink rate of 0.76 meter/second (2.5 ft/sec). This mechanization of the decoupled controller is desirable from the noise standpoint because the engines are automatically throttled back to approximately 35 percent of full power during the $6^{\circ}$ segment of the approach.

There was some concern, however, over the engine response characteristics in recovering from an engine failure when the throttles were at the 35-percent level. Consequently, a second mechanization was employed that used the horizontal tail, flaps, and symmetric spoilers as active control elements while keeping the throttle setting at the initial or trim value during the entire descent. The gains the pilots believed provided the best response are presented in table VII along with the resulting airplane stability characteristics. It should be noted that the pilot-induced oscillations due to the shortness of the phugoid period experienced with the unaugmented airplane (ref. 5) were never a problem with either of the decoupled control mechanizations. The time history of a typical flight performed with the second mechanization in turbulence with a rms gust intensity of

0.61 meter/second (2 ft/sec) is presented in figure 7. During this approach the pilot corrected for an initial lateral offset of 61 meters (200 ft) and landed within 3 meters (10 ft) of the runway center line in the designated landing area with a sink rate of about 1 meter/second (3 ft/sec). Although the pilots stated that no increase in difficulty was experienced when lateral offsets were included, numerous aileron and rudder inputs were made by the pilot. This mechanization is noisier than the first because the throttle is set at about 85 percent of full power for the entire descent and is less efficient because the spoilers must be uprigged by about $10^{\circ}$ to provide adequate flare capability.

The pilots were unable to detect any significant difference between the two mechanizations although there was more lift capability during flare when the throttle was used as an active control element. The pilots stated that they could obtain the desired glide slope more easily and with less workload using either version of the decoupled longitudinal controller than with the conventional controls and SAS. The pilots gave both mechanizations of the decoupled longitudinal controllers a pilot rating (PR) of 2 (table V) for the initial approach phase of operations, which was an improvement in PR of 1/2 increment over conventional controls with SAS. (See ref. 5.) The pilot ratings for the flare-to-landing maneuver were improved from $PR = 3$ to $PR = 2$ or better by using the decoupled controls, primarily because of the precision with which flight-path angle could be controlled in ground effects. The suckdown tendency experienced with conventional controls in ground effect was much less noticeable with the decoupled controls. The pilot rating of 2 for the flare-to-landing maneuver applies only to the two-segment approaches in which the flight-path angle of the final segment was $4^{\circ}$. As was the case with conventional controls, the pilot ratings degrade considerably as the final segment is steepened but are unaffected by increasing the initial glide slope from $6^{\circ}$ to $9^{\circ}$.

These pilot ratings are reflected in the touchdown conditions presented in table VIII in which the results obtained for the two research pilots and the research engineer are combined because no significant difference between pilots existed. The altitude and altitude-rate judgment problems that historically exist in simulations using closed-circuit television for image generation make the absolute magnitude of the sink rates attained in this study questionable. The sink rates at touchdown for visual simulations, however, are generally higher than those experienced in flight. Consequently, the results presented in table VIII should be conservative, and the relative values of sink rate obtained with the different control systems should provide a basis for comparison. The fact that the pilots had a tendency to land slightly long reflects the difficulty of the landing task. The research pilots stated, however, that important visual cues such as peripheral vision, depth perception, and resolution were lacking in the simulation and adversely affected their touchdown conditions as compared to actual landings. The pilots felt that the decoupled longitudinal control concept was a considerable improvement although the workload was still high in turbulence.

## Decoupled Lateral Controls

The decoupled-control concept was applied to the lateral control mode because much of the remaining workload was concerned with the lateral mode and because the lateral acceleration with conventional lateral controls with SAS (fig. 7) appeared to present a potential handling-qualities problem. The constant prefilter and feedback gains required for steady-state decoupled control of yaw rate $\dot{\psi}$ and sideslip angle $\beta$ were obtained (appendix B) in the same manner as the gains for decoupled longitudinal controls. In the simulation the decoupled lateral controls were mechanized so that the pilot used the wheel to control yaw rate and the pedals to control sideslip angle. In addition, the thumb button on the right horn of the wheel was mechanized to permit trim inputs to be made to sideslip angle.

The gains the pilots felt provided the best response are presented in table IX along with the resulting airplane stability characteristics. The time history of a typical flight in turbulence with a rms gust intensity of 0.61 meter/second (2 ft/sec) and a sustained crosswind of 12 knots is presented in figure 8. (The decoupled longitudinal controls used on this flight employ four active control elements which will be discussed in a subsequent section.) The airplane was initially trimmed in yaw to make a crabbed approach and was offset from the runway center line by 61 meters (200 ft). The pilot attained the center line of the runway using yaw-rate control and then applied sideslip control at an altitude of about 91.4 meters (300 ft) to remove the major crosswind effects while yawing to decrab and make a sideslipping final approach. The pilots could perform this type of crosswind approach in crosswinds up to 24 knots with no increase in difficulty or workload so long as the decrab maneuver was performed before the flare maneuver was required. Only one research pilot used the decoupled lateral controls and he gave them a PR = 2 primarily because of the reduced aircraft response to turbulence. (The reduction in lateral and rolling acceleration can be seen by comparing the results of figs. 7 and 8.) The pilot rating might have been even better had not the pilot felt that the improvement in response to turbulence may have resulted in a slightly sluggish lateral-control mode. The touchdown conditions attained using decoupled longitudinal and lateral controls are summarized in table X. The absence of degradation in touchdown conditions with increasing turbulence is indicative of the effectiveness of the decoupled lateral controls in reducing pilot workload in turbulence. An indirect comparison of lateral decoupled controls and conventional lateral controls with SAS can be made by comparing the results of table X with those of table VIII. The results shown in table X, however, are of a more difficult nature having been obtained in crosswinds up to 24 knots using both double- and single-segment glide slopes. The improvement in piloting performance with decoupled lateral controls primarily reflects an improvement in controller gains over those used in the conventional controls with SAS. The pilots felt, however, that the decoupled concept yielded no significant advantage in the lateral-control mode.

## Decelerating Approaches

When the pilot's task was altered to include decelerating from approximately 120 knots to 70 knots, the two mechanizations of the decoupled longitudinal controller previously discussed were not satisfactory. The primary problem was a large transient in flight-path angle that occurred when step inputs of 25 or 30 percent in forward velocity were made. The large transient in flight-path angle could be avoided by making gradual speed reductions. The potential danger at low altitudes, however, caused the pilots to give poor pilot ratings to these mechanizations. The undesirably large transients in flight-path angle were essentially eliminated by using all four active control elements – throttle, horizontal tail, flaps, and symmetric spoilers – in mechanizing approximately decoupled longitudinal controls (see appendix A). The gains the pilots believed provided the best response characteristics for this mechanization of the controls are presented in table XI as are the resulting airplane stability characteristics. These gains resulted in an approximately decoupled longitudinal controller that the pilots felt was as good or better for constant-speed approaches as the two mechanizations previously discussed. The decoupled longitudinal controller with four active elements was still deficient for making decelerating approaches because the flight-path angle sought a new trim value whenever forward velocity was changed. Although the thumb button on the left horn of the control wheel could be used to retrim the flight-path angle, an electrical pickoff was installed on the forward velocity control lever and employed in an automatic trim circuit for flight-path angle.

The response of this final mechanization of the decoupled steady-state controller is presented in figure 9. This figure illustrates how the flight-path angle changes due to rapidly commanded changes in pitch angle and forward velocity. In particular, $\gamma$ reaches a commanded value of $-5^{\circ}$ at 8 seconds and remains there except for small transients due to commanded pitch changes to $-4^{\circ}$ at 14 seconds, $3^{\circ}$ at 23 seconds, and $0^{\circ}$ at 34 seconds and a commanded velocity change of -8.9 knots (-15 ft/sec) at 41 seconds. The pitch angle $\theta$ changes only slightly when flight-path angle or forward velocity changes are commanded. The forward velocity experiences a steady-state change of roughly 1.2 knots (2 ft/sec) for a $5^{\circ}$ change in either pitch angle or flight-path angle. These responses are quite satisfactory. It is still desirable, however, to avoid abrupt changes in commanded velocity in the interests of passenger comfort and to avoid large excursions in throttle setting. (See fig. 10.) This decelerating approach, performed in zero turbulence, illustrates the precision with which flight-path angle can be controlled during a two-segment approach. The maximum variation of $\pm 1.5^{\circ}$ in flight-path angle occurred when the pilot made the step input in commanded forward velocity.

The time history of a decelerating approach during which the pilot set up the $6^{\circ}$ approach and then took approximately 20 seconds to reduce forward velocity from about 120 knots to 70 knots is presented in figure 11 for an rms gust intensity of 0.61 meter/second (2 ft/sec). The peak longitudinal acceleration during this flight was approximately 0.61 meter/second (2 ft/sec). When the commanded velocity was changed slowly, the flight-path angle varied only in response to turbulence. It should be noted that figure 11 shows high-frequency low-amplitude oscillations in $\delta_s$, $\dot{p}$, and $\dot{r}$. The gains used in this flight are not the best gains established in other flights and previously discussed (fig. 8) where such oscillations were eliminated. These oscillations were undetected by the pilot and hence did not affect the longitudinal control performance that was of major interest in this flight. In addition, when the final gains are used for the decoupled lateral controller, $\dot{p}$, $\dot{r}$, and $\delta_s$ do not oscillate. (See fig. 8.) The pilots believed that the four-control-element mechanization of the decoupled longitudinal controller yielded a very flyable airplane and gave it a PR = 3 or better for performing decelerating approaches. The touchdown conditions for decelerating approaches performed with decoupled lateral and longitudinal controls are summarized in table XII.

### Wave-Offs

During wave-offs the maintaining of pitch angle near zero by the decoupled longitudinal controls is an unnecessary restriction. The decoupled controls can be used, however, for wave-offs as indicated in figure 12. In this typical flight the pilot used flight-path angle control to go from level flight to a rate of climb of approximately 3.05 meters/second (10 ft/sec) in about 4 seconds. Care must be exercised in using this decoupled controller to command a velocity increase, however, because the resulting transient in flight-path angle can cause substantial sink rates. Consequently, any wave-off and climbout should be performed using $\gamma_c$ as the primary control, being careful to keep the angle of attack at an acceptable level and commanding an increase in forward velocity only after the desired rate of climb has been established. The tendency of a pilot trained on conventional controls to push the throttle lever full forward for an emergency wave-off combined with the tendency of the decoupled longitudinal controls to cause transients in sink rate when a velocity increase is commanded makes the use of the throttle lever to command forward velocity potentially very dangerous at low altitudes. Thus, it is probably desirable to use some lever other than the throttle lever to command forward velocity. In this case the throttle lever could be disengaged when the decoupled controllers were operating.

### Control Response Characteristics

Response characteristics for the decoupled longitudinal controls are different from those associated with conventional controls because the pitch angle $\theta_c$ is independent of the primary control $\gamma_c$. The time history presented in figure 9 shows typical responses. In this flight the pilot sets up a $5^0$ glide slope and after 14 seconds commands a pitch-angle change, reverses the command, and then removes the command. Although the aircraft pitch attitude response to these commands is fairly sluggish, the commanded change in flight-path angle $\gamma_c$ 60 seconds into the flight results in a change of $\gamma$ of approximately $5^{\circ}$ in about 1 second. In addition, the forward velocity was reduced by about 8.9 knots (15 ft/sec) in 3 seconds through the use of the velocity controller at 41 seconds into the flight.

In the lateral mode it is inappropriate to give characteristics associated with roll angle $\phi$ because the decoupled lateral controller does not have direct control over roll angle. The decoupled lateral controls provide independent control of yaw rate and sideslip angle and are capable of $t_{\Delta\psi=15^{\circ}} = 2$ seconds (a $15^{\circ}$ change in yaw in 2 sec) and $\Delta\psi_{t=1} = 7.2^{\circ}$ (requires 1 sec to change yaw angle by $7.2^{\circ}$). In addition, sideslip control requires approximately 5 seconds to change $\beta$ by $4^{\circ}$.

## CONCLUDING REMARKS

A fixed-base simulation study has been conducted to evaluate the use of decoupled controls as a means for reducing pilot workload during the approach and landing of an externally blown jet-flap STOL transport. The resulting decoupled longitudinal controller employed the throttle, horizontal tail, flaps, and symmetric spoilers as active control elements to provide steady-state decoupling of flight-path angle, pitch angle, and forward velocity. Requiring decoupled controls only in the steady-state case and restricting the controller to the approach and landing phase of operations permitted the use of constant prefilter and feedback gains in the decoupled control mechanization and avoided the need for an onboard computer. The piloting task was to use a localizer and flight director so as to capture and maintain a two-segment glide slope until landing in 137.2-meter-(450-ft) long area marked on the end of the runway.

### Decoupled Longitudinal Controls

In general, the pilots believed that the decoupled longitudinal control concept was an improvement over conventional controls. Specifically,

(1) The pilots could attain the desired glide slope more easily and with less workload using the decoupled controls. The decoupled controls were given a pilot rating of 2 for the initial approach phase of operation, an improvement of 1/2 increment over conventional controls.

(2) The pilot ratings for the flare-to-landing maneuver were improved from 3 to 2 with decoupled controls, primarily because of the precision with which flight-path angle could be controlled in ground effect.

(3) The pilot ratings for the flare maneuver become poorer as the flight-path angle of the second glide-slope segment of the approach increases above $4^{\circ}$ but are unaffected by increases in the initial glide-slope segment from $6^{\circ}$ to $9^{\circ}$.

(4) The decoupled longitudinal controls were given a pilot rating of 3 or better for making decelerating approaches from approximately 120 knots to 70 knots.

(5) The throttle lever was satisfactorily used as a velocity control lever in the current study; however, the tendency of a pilot trained on conventional controls to push the throttle lever full forward for an emergency wave-off combined with the tendency of the decoupled longitudinal controls to cause transients in sink rate when a velocity increase is commanded makes the use of the throttle lever to command forward velocity potentially dangerous at low altitudes. Consequently, it is probably desirable to use some lever other than the throttle lever to command forward velocity.

## Decoupled Lateral Controls

In an attempt to reduce pilot workload further, the spoilers, rudder, and ailerons were used to provide steady-state decoupling of yaw rate and sideslip angle. The pilots could land in crosswinds up to 24 knots and gave the decoupled lateral controls a pilot rating of 2. Improved pilot rating of the lateral-control mode with decoupled controls is primarily due to an improvement in controller gains over those used in conventional controls. The pilots felt that the decoupled concept yielded no significant advantage over conventional controls in the lateral mode.

Langley Research Center,
National Aeronautics and Space Administration,
Hampton, Va., November 7, 1973.

## APPENDIX A

## DECOUPLED LONGITUDINAL CONTROLS

The three longitudinal equations of motion were linearized as perturbations about an equilibrium condition in equations (1-59) of reference (7). These three equations can be nondimensionalized with respect to time using

$$t' = \frac{u_0}{c} t \tag{A1}$$

and solved simultaneously to give

$$\frac{d^2\theta'}{dt'^2} = \frac{1}{2\mu K_Y^2}\left[\left(\frac{C_{m_q} + C_{m_{\dot{\alpha}}}}{2}\right)\frac{d\theta'}{dt'} + \left(C_{m_\alpha} + \frac{C_{m_{\dot{\alpha}}} C_{Z_\alpha}}{4\mu}\right)\alpha' + \frac{C_{m_{\dot{\alpha}}} C_{Z_u}}{4\mu} u' + \left(C_{m_{\delta_t}} + \frac{C_{m_{\dot{\alpha}}} C_{Z_{\delta_t}}}{4\mu}\right)\delta_t' + \left(C_{m_{\delta_{\overline{f3}}}} + \frac{C_{m_{\dot{\alpha}}} C_{Z_{\delta_{\overline{f3}}}}}{4\mu}\right)\delta_{\overline{f3}}' + \left(C_{m_{\delta_{sp}}} + \frac{C_{m_{\dot{\alpha}}} C_{Z_{\delta_{sp}}}}{4\mu}\right)\delta_{sp}'\right] \tag{A2}$$

$$\frac{d\alpha'}{dt'} = \frac{1}{2\mu}\left(2\mu \frac{d\theta'}{dt'} + C_{Z_\alpha}\alpha' + C_{Z_u}u' + C_{Z_{\delta_t}}\delta_t' + C_{Z_{\delta_{\overline{f3}}}}\delta_{\overline{f3}}' + C_{Z_{\delta_{sp}}}\delta_{sp}'\right) \tag{A3}$$

$$\frac{du'}{dt'} = \frac{1}{2\mu}\left[C_W\theta' + \left(\frac{C_{X_q} + C_{X_{\dot{\alpha}}}}{2}\right)\frac{d\theta'}{dt'} + \left(C_{X_\alpha} + \frac{C_{X_{\dot{\alpha}}} C_{Z_\alpha}}{4\mu}\right)\alpha' + \left(C_{X_u} + \frac{C_{X_{\dot{\alpha}}} C_{Z_u}}{4\mu}\right)u' + \left(C_T + \frac{C_{X_{\dot{\alpha}}} C_{Z_{\delta_{th}}}}{4\mu}\right)\delta_{th}' + \left(C_{X_{\delta_t}} + \frac{C_{X_{\dot{\alpha}}} C_{Z_{\delta_t}}}{4\mu}\right)\delta_t' + \left(C_{X_{\delta_{\overline{f3}}}} + \frac{C_{X_{\dot{\alpha}}} C_{Z_{\delta_{\overline{f3}}}}}{4\mu}\right)\delta_{\overline{f3}}' + \left(C_{X_{\delta_{sp}}} + \frac{C_{X_{\dot{\alpha}}} C_{Z_{\delta_{sp}}}}{4\mu}\right)\delta_{sp}'\right] \tag{A4}$$

where the primed parameters are perturbations from the equilibrium or trim conditions of the airplane in nondimensional form; that is

$$\theta' = \theta - \theta_0 \tag{A5}$$

$$\alpha' = \alpha - \alpha_0 = \frac{w - w_0}{u_0} \tag{A6}$$

$$u' = \frac{u - u_0}{u_0} \tag{A7}$$

and where

$$\mu = \frac{m}{\rho S c} \tag{A8}$$

$$K_Y{}^2 = \frac{I_Y}{mc^2} \tag{A9}$$

The mass and dimensional characteristics of the simulated airplane are presented in table II and the basic aerodynamic coefficients in table III. Constant coefficients were employed in the linearized longitudinal equations of motion corresponding to an angle of attack of $5^{\circ}$, a forward velocity of 70 knots, and a thrust coefficient $C_T$ of 1.87.

The linearized longitudinal equations of motion can be written in state vector notation as

$$\dot{\bar{x}} = A\bar{x} + B\bar{u} \tag{A10}$$

where the state vector is

$$\bar{x} = \begin{bmatrix} \theta' \\ \dot{\theta}' \\ \alpha' \\ u' \end{bmatrix} \tag{A11}$$

and the control vector is

$$\bar{u} = \begin{bmatrix} \delta'_{th} \\ \delta_t' \\ \delta'_{\overline{f3}} \\ \delta'_{sp} \end{bmatrix} \tag{A12}$$

The general control law is given as

$$\bar{u} = -F\bar{x} + G\bar{r} \tag{A13}$$

where $\bar{r}$ is the vector of commanded-pilot inputs $\gamma_c$, $\theta_c$, and $u_c$ that are to be controlled in a decoupled manner. The output equation is

$$\bar{y} = C\bar{x} \tag{A14}$$

When equation (A13) is substituted into equation (A10), the Laplace transform of the result can be written as

$$\bar{x}(s) = (sI - A + BF)^{-1}BG\bar{r}(s) \tag{A15}$$

Substituting the Laplace transform of equation (A14) into equation (A15) and requiring that the output $\bar{y}(s)$ be equal to the commanded-pilot input $\bar{r}(s)$ under steady-state conditions results in the prefilter gain

$$G = -\left[C(A - BF)^{-1}B\right]^{-1} \tag{A16}$$

Normally the bracketed term is nonsingular. There are cases, however, when all four control elements are used to decouple flight-path angle, pitch angle, and forward velocity, so that the bracketed term is singular. In this case the difference between the actual output $\bar{y}(s)$ and the commanded-pilot input $\bar{r}(s)$ is minimized (approximately decoupled steady-state control) by using the pseudo inverse of $C(A - BF)^{-1}B$. Because this term has zeros in the fourth row, it can be written

$$C(A - BF)^{-1}B = TN \tag{A17}$$

where

$$T = \begin{bmatrix} 100 \\ 010 \\ 001 \\ 000 \end{bmatrix} \tag{A18}$$

and N is $C(A - BF)^{-1}B$ with the fourth row deleted. The pseudo inverse can then be written (ref. 8) as

$$G = -N^T\left(NN^T\right)^{-1}T^T \tag{A19}$$

Having obtained the prefilter gain matrix G required for approximately decoupled steady-state control, it is desirable to obtain the control that will reach that condition as efficiently as possible. Consequently optimal control theory was employed to obtain the feedback gain matrix F.

For a given constant-pilot input $\bar{r}$ there is an associated equilibrium state $\bar{x}_e$ that is reached in the steady-state case; that is

$$0 = (A - BF)\bar{x}_e + BG\bar{r} \tag{A20}$$

which, since it is zero, can be subtracted from the closed-loop equations of motion,

$$\dot{\hat{x}} = (A - BF)\bar{x} + BG\bar{r} - \left[(A - BF)\bar{x}_e + BG\bar{r}\right] \tag{A21}$$

where $\hat{x}$ is the difference between the instantaneous state and the new equilibrium state, $\bar{x} - \bar{x}_e$. Equation (A21) is therefore

$$\dot{\hat{x}} = (A - BF)\hat{x} \tag{A22}$$

which can be written as

$$\dot{\hat{x}} = A\hat{x} + B\hat{u} \tag{A23}$$

where

$$\hat{u} = -F\hat{x} \tag{A24}$$

the difference between the instantaneous control vector $\bar{u}$ and the pilot-control input associated with the new equilibrium state. The performance index

$$J = \int_0^\infty \left(\hat{x}^T Q \hat{x} + \hat{u}^T R \hat{u}\right) dt \tag{A25}$$

together with equation (A23) constitutes the familiar state-regulator problem with quadratic performance index for which the optimal control (ref. 9) is

$$\hat{u}^* = -R^{-1}B^T P\hat{x} \tag{A26}$$

where $P$ is the solution to the time invariant matrix Riccati equation

$$PA + A^T P - PBR^{-1}B^T P + Q = 0 \tag{A27}$$

The particular solution for the Riccati equation is based on the iterative approach taken in reference 10.

Equating the general control $\hat{u}$ to the optimal $\hat{u}^*$ permits the solution for the remaining unknown gain matrix

$$F = R^{-1}B^T P \tag{A28}$$

The feedback gain $F$ is optimal for a given set of weighting matrices $Q$ and $R$ in the performance index (eq. (A25)). The off-diagonal terms in these weighting matrices were zero while the diagonal terms were varied as a function of pilot opinion, as the simulation study progressed.

## APPENDIX B

## DECOUPLED LATERAL CONTROLS

The lateral equations of motion were linearized as perturbations about an equilibrium condition (ref. 7) as

$$\frac{d^2\phi'}{dt'^2} = \frac{cmb}{2\mu I_{XZ}}\left\{\frac{b}{2c}\left[\left(\frac{I_Z I_{XZ}}{I_Z{}^2 - I_{XZ}^2}\right)C_{l_p} + \left(\frac{I_Z I_X}{I_Z{}^2 - I_{XZ}^2} - 1\right)C_{n_p}\right]\frac{d\phi'}{dt'} + \frac{b}{2c}\left[\left(\frac{I_Z I_{XZ}}{I_Z{}^2 - I_{XZ}^2}\right)C_{l_r}\right.\right.$$

$$\left. + \left(\frac{I_Z I_X}{I_Z{}^2 - I_{XZ}^2} - 1\right)C_{n_r}\right]\frac{d\psi'}{dt'} + \left[\left(\frac{I_Z I_{XZ}}{I_Z{}^2 - I_{XZ}^2}\right)C_{l_\beta} + \left(\frac{I_Z I_X}{I_Z{}^2 - I_{XZ}^2} - 1\right)C_{n_\beta}\right]\beta'$$

$$+ \left[\left(\frac{I_Z I_{XZ}}{I_Z{}^2 - I_{XZ}^2}\right)C_{l_{\delta_r}} + \left(\frac{I_Z I_X}{I_Z{}^2 - I_{XZ}^2} - 1\right)C_{n_{\delta_r}}\right]\delta_r' + \left[\left(\frac{I_Z I_{XZ}}{I_Z{}^2 - I_{XZ}^2}\right)C_{l_{\delta_a}}\right.$$

$$\left.\left. + \left(\frac{I_Z I_X}{I_Z{}^2 - I_{XZ}^2} - 1\right)C_{n_{\delta_a}}\right]\delta_a' + \left[\left(\frac{I_Z I_{XZ}}{I_Z{}^2 - I_{XZ}^2}\right)C_{l_{\delta_s}} + \left(\frac{I_Z I_X}{I_Z{}^2 - I_{XZ}^2} - 1\right)C_{n_{\delta_s}}\right]\delta_s'\right\} \tag{B1}$$

$$\frac{d^2\psi'}{dt'^2} = \frac{cmb}{2\mu\left(I_Z{}^2 - I_{XZ}^2\right)}\left[\frac{b}{2c}\left(I_{XZ}C_{l_p} + I_X C_{n_p}\right)\frac{d\phi'}{dt'} + \frac{b}{2c}\left(I_{XZ}C_{l_r} + I_X C_{n_r}\right)\frac{d\psi'}{dt'} + \left(I_{XZ}C_{l_\beta}\right.\right.$$

$$\left. + I_X C_{n_\beta}\right)\beta' + \left(I_{XZ}C_{l_{\delta_r}} + I_X C_{n_{\delta_r}}\right)\delta_r' + \left(I_{XZ}C_{l_{\delta_a}} + I_X C_{n_{\delta_a}}\right)\delta_a'$$

$$\left. + \left(I_{XZ}C_{l_{\delta_s}} + I_X C_{n_{\delta_s}}\right)\delta_s'\right] \tag{B2}$$

$$\frac{d\beta'}{dt'} = \frac{1}{2\mu}\left[C_{Y_\phi}\phi' + \frac{b}{2c}C_{Y_p}\frac{d\phi'}{dt'} + \left(\frac{b}{2c}C_{Y_r} - 2\mu\right)\frac{d\psi'}{dt'} + C_{Y_\beta}\beta' + C_{Y_{\delta_r}}\delta_r' \right.$$

$$\left. + C_{Y_{\delta_a}}\delta_a' + C_{Y_{\delta_s}}\delta_s'\right] \tag{B3}$$

where the primed parameters are perturbations from equilibrium conditions with

$$t' = \frac{u_0}{c}t \tag{B4}$$

$$\mu = \frac{m}{\rho s_c} \tag{B5}$$

These linearized lateral equations of motion are then written in state vector notation

$$\dot{\bar{x}} = A\bar{x} + B\bar{u} \tag{B6}$$

and the prefilter and feedback gain matrices required to decouple yaw rate and sideslip angle are determined as in appendix A.

## REFERENCES


1. Parlett, Lysle P.; Greer, H. Douglas; Henderson, Robert L.; and Carter, C. Robert: Wind-Tunnel Investigation of an External-Flow Jet-Flap Transport Configuration Having Full-Span Triple-Slotted Flaps. NASA TN D-6391, 1971.

2. Grafton, Sue B.; Parlett, Lysle P.; and Smith, Charles C., Jr.: Dynamic Stability Derivatives of a Jet Transport Configuration With High Thrust-Weight Ratio and an Externally Blown Jet Flap. NASA TN D-6440, 1971.

3. Vogler, Raymond D.: Wind-Tunnel Investigation of a Four-Engine Externally Blowing Jet-Flap STOL Airplane Model. NASA TN D-7034, 1970.

4. Grantham, William D.; Sommer, Robert W.; and Deal, Perry L.: Simulator Study of Flight Characteristics of a Jet-Flap STOL Transport Airplane During Approach and Landing. NASA TN D-6225, 1971.

5. Grantham, William D.; Nguyen, Luat T.; Patton, James M., Jr.; Deal, Perry L.; Champine, Robert A.; and Carter, C. Robert: Fixed-Base Simulator Study of an Externally Blown Flap STOL Transport Airplane During Approach and Landing. NASA TN D-6898, 1972.

6. Kaestner, P. T.: An Articulated Optical Pickup for Scale Model Simulation. J. SMPTE, vol. 76, no. 10, Oct. 1967, pp. 988-991.

7. Blakeloch, John H.: Automatic Control of Aircraft and Missiles. John Wiley & Sons, Inc., c.1965.

8. Zadeh, Lotfi A.; and Desoer, Charles A.: Linear System Theory. McGraw-Hill Book Co., Inc., c.1963.

9. Athans, Michael; and Falb, Peter L.: Optimal Control. McGraw-Hill Book Co., Inc., c.1966.

10. Kleinman, David L.: On an Iterative Technique for Riccati Equation Computations. IEEE Trans. Automat. Contr., vol. AC-13, no. 1, Feb. 1968, pp. 114-115.

TABLE I.- SIMULATED ENGINE RESPONSE CHARACTERISTICS

[The thrust values are presented in units of newtons (pounds force)]

(a) Acceleration

| Time, sec | Thrust response for $T_c$, N (lbf), of – | | | | | | | | | | |
|---|---|---|---|---|---|---|---|---|---|---|---|
| | 2611 (587) | 6530 (1468) | 13 625 (3063) | 16 796 (3776) | 22 023 (4951) | 36 764 (8265) | 6904 (1552) | 14 741 (3314) | 18 847 (4237) | 21 649 (4867) | 36 764 (8265) |
| 0 | 1681 (378) | 1681 ( 378) | 1 681 ( 378) | 1 681 ( 378) | 1 681 ( 378) | 1 681 ( 378) | 2611 ( 587) | 2 611 ( 587) | 2 611 ( 587) | 2 611 ( 587) | 2 611 ( 587) |
| .2 | 1681 (378) | 1681 ( 378) | 1 681 ( 378) | 1 681 ( 378) | 1 681 ( 378) | 1 681 ( 378) | 2705 ( 608) | 2 705 ( 608) | 2 705 ( 608) | 2 705 ( 608) | 2 705 ( 608) |
| .4 | 1775 (399) | 1775 ( 399) | 1 775 ( 399) | 1 775 ( 399) | 1 775 ( 399) | 1 775 ( 399) | 2798 ( 629) | 2 798 ( 629) | 2 798 ( 629) | 2 798 ( 629) | 2 798 ( 629) |
| .6 | 1868 (420) | 1868 ( 420) | 1 868 ( 420) | 1 868 ( 420) | 1 868 ( 420) | 1 868 ( 420) | 2985 ( 671) | 2 985 ( 671) | 2 985 ( 671) | 2 985 ( 671) | 2 985 ( 671) |
| .8 | 2055 (462) | 2055 ( 462) | 2 055 ( 462) | 2 055 ( 462) | 2 055 ( 462) | 2 055 ( 462) | 3358 ( 755) | 3 358 ( 755) | 3 358 ( 755) | 3 358 ( 755) | 3 358 ( 755) |
| 1.0 | 2144 (482) | 2144 ( 482) | 2 144 ( 482) | 2 144 ( 482) | 2 144 ( 482) | 2 144 ( 482) | 4106 ( 923) | 4 106 ( 923) | 4 106 ( 923) | 4 106 ( 923) | 4 106 ( 923) |
| 1.2 | 2331 (524) | 2331 ( 524) | 2 331 ( 524) | 2 331 ( 524) | 2 331 ( 524) | 2 331 ( 524) | 5227 (1175) | 5 227 (1175) | 5 227 (1175) | 5 227 (1175) | 5 227 (1175) |
| 1.4 | 2424 (545) | 2611 ( 587) | 2 611 ( 587) | 2 611 ( 587) | 2 611 ( 587) | 2 611 ( 587) | 5600 (1259) | 7 090 (1594) | 7 277 (1636) | 7 277 (1636) | 7 277 (1636) |
| 1.6 | 2518 (566) | 2985 ( 671) | 2 985 ( 671) | 2 985 ( 671) | 2 985 ( 671) | 2 985 ( 671) | 5880 (1322) | 10 449 (2349) | 10 449 (2349) | 10 449 (2349) | 10 449 (2349) |
| 1.8 | 2611 (587) | 3545 ( 797) | 3 545 ( 797) | 3 545 ( 797) | 3 545 ( 797) | 3 545 ( 797) | 6161 (1385) | 11 196 (2517) | 12 691 (2853) | 12 691 (2853) | 15 302 (3440) |
| 2.0 | | 4012 ( 902) | 4 386 ( 986) | 4 386 ( 986) | 4 386 ( 986) | 4 386 ( 986) | 6343 (1426) | 11 943 (2685) | 14 372 (3231) | 15 115 (3398) | 18 473 (4153) |
| 2.2 | | 4666 (1049) | 5 600 (1259) | 5 600 (1259) | 5 600 (1259) | 5 600 (1259) | 6437 (1447) | 12 504 (2811) | 15 489 (3482) | 16 796 (3776) | 21 649 (4867) |
| 2.4 | | 5040 (1133) | 8 211 (1846) | 8 211 (1846) | 8 211 (1846) | 8 211 (1846) | 6623 (1489) | 12 878 (2895) | 16 329 (3671) | 17 917 (4028) | 24 447 (5496) |
| 2.6 | | 5600 (1259) | 9 519 (2140) | 11 383 (2559) | 11 383 (2559) | 11 383 (2559) | 6717 (1510) | 13 158 (2958) | 16 983 (3818) | 18 571 (4175) | 26 876 (6042) |
| 2.8 | | 5974 (1343) | 10 360 (2329) | 12 686 (2852) | 15 395 (3461) | 16 610 (3734) | 6810 (1531) | 13 438 (3021) | 17 357 (3902) | 19 034 (4279) | 28 740 (6461) |
| 3.0 | | 6250 (1405) | 11 196 (2517) | 13 812 (3105) | 16 983 (3818) | 21 276 (4783) | 6904 (1552) | 13 625 (3063) | 17 637 (3965) | 19 407 (4363) | 30 048 (6755) |
| 3.2 | | 6437 (1447) | 11 943 (2685) | 14 741 (3314) | 18 104 (4070) | 24 634 (5538) | | 13 718 (3084) | 17 824 (4007) | 19 781 (4447) | 31 258 (7027) |
| 3.4 | | 6530 (1468) | 12 317 (2769) | 15 302 (3440) | 18 571 (4175) | 27 619 (6209) | | 13 905 (3126) | 18 011 (4049) | 19 968 (4489) | 32 378 (7279) |
| 3.6 | | | 12 691 (2853) | 15 675 (3524) | 19 034 (4279) | 29 487 (6629) | | 13 998 (3147) | 18 104 (4070) | 20 248 (4552) | 33 126 (7447) |
| 3.8 | | | 12 878 (2895) | 15 956 (3587) | 19 407 (4363) | 31 164 (7006) | | 14 092 (3168) | 18 198 (4091) | 20 417 (4590) | 33 780 (7594) |
| 4.0 | | | 13 251 (2979) | 16 143 (3629) | 19 781 (4447) | 32 472 (7300) | | 14 185 (3189) | 18 384 (4133) | 20 715 (4657) | 34 340 (7720) |
| 4.2 | | | 13 438 (3021) | 16 236 (3650) | 20 061 (4510) | 33 499 (7531) | | 14 279 (3210) | 18 473 (4153) | 20 809 (4678) | 34 807 (7825) |
| 4.4 | | | 13 625 (3063) | 16 423 (3692) | 20 342 (4573) | 34 153 (7678) | | 14 372 (3231) | 18 571 (4175) | 20 996 (4720) | 35 270 (7929) |
| 4.6 | | | | 16 516 (3713) | 20 435 (4594) | 34 714 (7804) | | 14 466 (3252) | 18 665 (4196) | 21 089 (4741) | 35 643 (8013) |
| 4.8 | | | | 16 610 (3734) | 20 622 (4636) | 35 270 (7929) | | 14 555 (3272) | 18 754 (4216) | 21 182 (4762) | 35 924 (8076) |
| 5.0 | | | | 16 703 (3755) | 20 715 (4657) | 35 643 (8013) | | 14 648 (3293) | 18 847 (4237) | 21 276 (4783) | 36 204 (8139) |
| 5.2 | | | | 16 796 (3776) | 20 902 (4699) | 36 017 (8097) | | 14 741 (3314) | | 21 463 (4825) | 36 391 (8181) |
| 5.4 | | | | | 20 996 (4720) | 36 297 (8160) | | | | 21 556 (4846) | 36 578 (8223) |
| 5.6 | | | | | 21 089 (4741) | 36 578 (8223) | | | | 21 649 (4867) | 36 671 (8244) |
| 5.8 | | | | | 21 276 (4783) | 36 671 (8244) | | | | | 36 764 (8265) |
| 6.0 | | | | | 21 463 (4825) | 36 764 (8265) | | | | | |
| 6.2 | | | | | 21 556 (4846) | | | | | | |
| 6.4 | | | | | 21 649 (4867) | | | | | | |
| 6.6 | | | | | 21 930 (4930) | | | | | | |
| 6.8 | | | | | 22 023 (4951) | | | | | | |

TABLE I.- SIMULATED ENGINE RESPONSE CHARACTERISTICS – Continued

[The thrust values are presented in units of newtons (pounds force)]

(a) Acceleration – Concluded

| Time, sec | Thrust response for $T_c$, N (lbf), of – | | | | | | | | | | | |
|---|---|---|---|---|---|---|---|---|---|---|---|---|
| | 36 764 (8265) | 18 198 (4091) | 36 764 (8265) | 13 905 (3126) | 22 397 (5035) | 36 764 (8265) | 19 594 (4405) | 22 953 (5160) | 36 764 (8265) | 22 953 (5160) | 36 764 (8265) | 36 764 (8265) |
| 0 | 4 479 (1007) | 11 196 (2517) | 11 196 (2517) | 12 317 (2769) | 12 317 (2769) | 12 317 (2769) | 16 796 (3776) | 16 796 (3776) | 16 796 (3776) | 20 715 (4657) | 20 715 (4657) | 24 447 (5496) |
| .2 | 4 853 (1091) | 12 317 (2769) | 12 317 (2769) | 12 878 (2895) | 13 998 (3147) | 13 998 (3147) | 18 291 (4112) | 19 221 (4321) | 19 221 (4321) | 21 836 (4909) | 24 074 (5412) | 27 806 (6251) |
| .4 | 5 600 (1259) | 14 555 (3272) | 15 675 (3524) | 13 251 (2979) | 16 796 (3776) | 16 796 (3776) | 18 940 (4258) | 20 342 (4573) | 24 074 (5412) | 22 116 (4972) | 30 048 (6755) | 31 912 (7174) |
| .6 | 7 090 (1594) | 15 302 (3440) | 20 528 (4615) | 13 438 (3021) | 18 291 (4112) | 22 397 (5035) | 19 127 (4300) | 21 089 (4741) | 27 993 (6293) | 22 303 (5014) | 32 472 (7300) | 33 407 (7510) |
| .8 | 9 519 (2140) | 16 049 (3608) | 24 634 (5538) | 13 531 (3042) | 19 407 (4363) | 26 129 (5874) | 19 407 (4363) | 21 836 (4909) | 30 608 (6881) | 22 490 (5056) | 33 780 (7594) | 34 528 (7762) |
| 1.0 | 12 878 (2895) | 16 610 (3734) | 27 993 (6293) | 13 625 (3063) | 20 342 (4573) | 29 113 (6545) | 19 594 (4405) | 22 397 (5035) | 32 472 (7300) | 22 677 (5098) | 34 527 (7762) | 35 644 (8013) |
| 1.2 | 17 917 (4028) | 17 170 (3860) | 30 234 (6797) | 13 718 (3084) | 20 902 (4699) | 30 888 (6944) | | 22 677 (5098) | 33 593 (7552) | 22 770 (5119) | 35 087 (7888) | 36 205 (8139) |
| 1.4 | 22 397 (5035) | 17 357 (3902) | 31 538 (7090) | 13 812 (3105) | 21 463 (4825) | 32 285 (7258) | | 22 953 (5160) | 34 247 (7699) | 22 953 (5160) | 35 643 (8013) | 36 764 (8265) |
| 1.6 | 25 755 (5790) | 17 637 (3965) | 32 472 (7300) | 13 905 (3126) | 21 930 (4930) | 33 219 (7468) | | | 34 714 (7804) | | 36 017 (8097) | |
| 1.8 | 28 553 (6419) | 17 917 (4028) | 33 219 (7468) | | 22 210 (4993) | 33 966 (7636) | | | 35 270 (7929) | | 36 391 (8181) | |
| 2.0 | 30 421 (6839) | 18 011 (4049) | 33 780 (7594) | | 22 397 (5035) | 34 527 (7762) | | | 35 830 (8055) | | 36 764 (8265) | |
| 2.2 | 31 444 (7069) | 18 104 (4070) | 34 340 (7720) | | | 35 087 (7888) | | | 36 204 (8139) | | | |
| 2.4 | 32 285 (7258) | 18 198 (4091) | 34 714 (7804) | | | 35 457 (7971) | | | 36 578 (8223) | | | |
| 2.6 | 32 846 (7384) | | 35 270 (7929) | | | 35 830 (8055) | | | 36 764 (8265) | | | |
| 2.8 | 33 499 (7531) | | 35 830 (8055) | | | 36 297 (8160) | | | | | | |
| 3.0 | 34 153 (7678) | | 36 204 (8139) | | | 36 578 (8223) | | | | | | |
| 3.2 | 34 714 (7804) | | 36 484 (8202) | | | 36 764 (8265) | | | | | | |
| 3.4 | 35 087 (7888) | | 36 671 (8244) | | | | | | | | | |
| 3.6 | 35 457 (7971) | | 36 764 (8265) | | | | | | | | | |
| 3.8 | 35 737 (8034) | | | | | | | | | | | |
| 4.0 | 35 924 (8076) | | | | | | | | | | | |
| 4.2 | 36 110 (8118) | | | | | | | | | | | |
| 4.4 | 36 204 (8139) | | | | | | | | | | | |
| 4.6 | 36 391 (8181) | | | | | | | | | | | |
| 4.8 | 36 484 (8202) | | | | | | | | | | | |
| 5.0 | 36 578 (8223) | | | | | | | | | | | |
| 5.2 | 36 671 (8244) | | | | | | | | | | | |
| 5.4 | 36 764 (8265) | | | | | | | | | | | |

TABLE I.- SIMULATED ENGINE RESPONSE CHARACTERISTICS – Continued

[The thrust values are presented in units of newtons (pounds force)]

(b) Deceleration

| Time, sec | Thrust response for $T_c$, N (lbf), of – | | | | | | | | | |
|---|---|---|---|---|---|---|---|---|---|---|
| | 1 681 ( 378) | 8 772 (1972) | 17 357 (3902) | 19 781 (4447) | 24 447 (5496) | 1 681 ( 378) | 13 069 (2938) | 16 796 (3776) | 21 836 (4909) | 1 681 ( 378) |
| 0 | 36 764 (8265) | 36 764 (8265) | 36 764 (8265) | 36 764 (8265) | 36 764 (8265) | 24 634 (5538) | 24 634 (5538) | 24 634 (5538) | 23 513 (5286) | 22 770 (5119) |
| .2 | 32 846 (7384) | 32 846 (7384) | 32 846 (7384) | 32 846 (7384) | 32 846 (7384) | 21 743 (4888) | 21 743 (4888) | 22 210 (4993) | 23 046 (5181) | 20 155 (4531) |
| .4 | 26 876 (6042) | 26 876 (6042) | 26 876 (6042) | 26 876 (6042) | 26 876 (6042) | 19 221 (4321) | 19 221 (4321) | 20 155 (4531) | 22 677 (5098) | 18 198 (4091) |
| .6 | 22 397 (5035) | 22 397 (5035) | 24 447 (5496) | 24 634 (5538) | 24 634 (5538) | 17 170 (3860) | 17 170 (3860) | 19 034 (4279) | 22 397 (5035) | 16 049 (3608) |
| .8 | 18 847 (4237) | 18 847 (4237) | 22 584 (5077) | 23 700 (5328) | 24 447 (5496) | 15 675 (3524) | 15 675 (3524) | 18 478 (4154) | 22 210 (4993) | 13 998 (3147) |
| 1.0 | 16 610 (3734) | 16 610 (3734) | 21 463 (4825) | 23 140 (5202) | | 14 092 (3168) | 15 022 (3377) | 18 104 (4070) | 22 116 (4972) | 12 504 (2811) |
| 1.2 | 14 928 (3356) | 15 302 (3440) | 21 099 (4741) | 22 770 (5119) | | 12 691 (2853) | 14 555 (3272) | 17 824 (4007) | 21 930 (4930) | 11 290 (2538) |
| 1.4 | 13 812 (3105) | 14 372 (3231) | 20 715 (4657) | 22 397 (5035) | | 11 196 (2517) | 14 092 (3168) | 17 637 (3965) | 21 836 (4909) | 10 449 (2349) |
| 1.6 | 12 504 (2811) | 13 812 (3105) | 20 342 (4573) | 22 210 (4993) | | 10 449 (2349) | 13 812 (3105) | 17 450 (3923) | | 9 706 (2182) |
| 1.8 | 11 570 (2601) | 13 438 (3021) | 19 968 (4489) | 22 023 (4951) | | 9 519 (2140) | 13 438 (3021) | 17 357 (3902) | | 8 959 (2014) |
| 2.0 | 10 916 (2454) | 12 971 (2916) | 19 594 (4405) | 21 836 (4909) | | 8 772 (1972) | 13 251 (2979) | 17 263 (3881) | | 8 398 (1888) |
| 2.2 | 10 266 (2308) | 12 691 (2853) | 19 221 (4321) | 21 649 (4867) | | 8 211 (1846) | 13 069 (2938) | 17 170 (3860) | | 7 838 (1762) |
| 2.4 | 9 519 (2140) | 12 410 (2790) | 19 034 (4279) | 21 463 (4825) | | 7 838 (1762) | | 17 077 (3839) | | 7 277 (1636) |
| 2.6 | 8 772 (1972) | 12 130 (2727) | 18 847 (4237) | 21 276 (4783) | | 7 371 (1657) | | 16 983 (3818) | | 6 904 (1552) |
| 2.8 | 8 211 (1846) | 11 943 (2685) | 18 665 (4196) | 21 089 (4741) | | 6 997 (1573) | | 16 890 (3797) | | 6 530 (1468) |
| 3.0 | 7 838 (1762) | 11 663 (2622) | 18 478 (4154) | 20 902 (4699) | | 6 717 (1510) | | 16 796 (3776) | | 6 161 (1385) |
| 3.2 | 7 464 (1678) | 11 476 (2580) | 18 291 (4112) | 20 809 (4678) | | 6 343 (1426) | | | | 5 787 (1301) |
| 3.4 | 7 090 (1594) | 11 290 (2538) | 18 198 (4091) | 20 715 (4657) | | 5 974 (1343) | | | | 5 600 (1259) |
| 3.6 | 6 717 (1510) | 11 103 (2496) | 18 104 (4070) | 20 528 (4615) | | 5 600 (1259) | | | | 5 320 (1196) |
| 3.8 | 6 530 (1468) | 11 009 (2475) | 18 011 (4049) | 20 435 (4594) | | 5 413 (1217) | | | | 5 133 (1154) |
| 4.0 | 6 161 (1385) | 10 822 (2433) | 17 917 (4028) | 20 342 (4573) | | 5 227 (1175) | | | | 4 853 (1091) |
| 4.2 | 5 974 (1343) | 10 636 (2391) | 17 824 (4007) | 20 248 (4552) | | 5 040 (1133) | | | | 4 573 (1028) |
| 4.4 | 5 694 (1280) | 10 449 (2349) | 17 731 (3986) | 20 155 (4531) | | 4 760 (1070) | | | | 4 386 ( 986) |
| 4.6 | 5 413 (1217) | 10 360 (2329) | 17 637 (3965) | 20 061 (4510) | | 4 479 (1007) | | | | 4 106 ( 923) |
| 4.8 | 5 227 (1175) | 10 266 (2308) | 17 544 (3944) | 19 968 (4489) | | 4 293 ( 965) | | | | 3 825 ( 860) |
| 5.0 | 5 040 (1133) | 10 080 (2266) | 17 450 (3923) | 19 875 (4468) | | 4 107 ( 923) | | | | 3 639 ( 818) |
| 5.2 | 4 853 (1091) | 9 986 (2245) | 17 357 (3902) | 19 781 (4447) | | 3 732 ( 839) | | | | 3 452 ( 776) |
| 5.4 | 4 479 (1007) | 9 893 (2224) | | | | 3 545 ( 797) | | | | 3 265 ( 734) |
| 5.6 | 4 293 ( 965) | 9 706 (2182) | | | | 3 358 ( 755) | | | | 3 172 ( 713) |
| 5.8 | 4 106 ( 923) | 9 613 (2161) | | | | 3 265 ( 734) | | | | 2 985 ( 671) |
| 6.0 | 3 919 ( 881) | 9 519 (2140) | | | | 3 078 ( 692) | | | | 2 798 ( 629) |
| 6.2 | 3 732 ( 839) | 9 426 (2119) | | | | 2 985 ( 671) | | | | 2 705 ( 608) |
| 6.4 | 3 545 ( 797) | 9 239 (2077) | | | | 2 798 ( 629) | | | | 2 518 ( 566) |
| 6.6 | 3 172 ( 713) | 9 145 (2056) | | | | 2 611 ( 587) | | | | 2 424 ( 545) |
| 6.8 | 2 985 ( 671) | 9 052 (2035) | | | | 2 424 ( 545) | | | | 2 237 ( 503) |
| 7.0 | 2 798 ( 629) | 8 959 (2014) | | | | 2 237 ( 503) | | | | 2 055 ( 462) |
| 7.2 | 2 611 ( 587) | 8 865 (1993) | | | | 2 055 ( 462) | | | | 1 962 ( 441) |
| 7.4 | 2 424 ( 545) | 8 772 (1972) | | | | 1 868 ( 420) | | | | 1 868 ( 420) |
| 7.6 | 2 144 ( 482) | | | | | 1 681 ( 378) | | | | 1 775 ( 399) |
| 7.8 | 1 868 ( 420) | | | | | | | | | 1 681 ( 378) |
| 8.0 | 1 681 ( 378) | | | | | | | | | |

TABLE I.- SIMULATED ENGINE RESPONSE CHARACTERISTICS – Concluded

[The thrust values are presented in units of newtons (pounds force)]

(b) Deceleration – Concluded

| Time, sec | Thrust response for $T_c$, N (lbf), of – | | | | | | | | | |
|---|---|---|---|---|---|---|---|---|---|---|
| | 3 732 ( 839) | 17 917 (4028) | 11 917 (2679) | 1 681 ( 378) | 7 464 (1678) | 3 732 ( 839) | 12 691 (2853) | 1 681 ( 378) | 3732 ( 839) | 1681 ( 378) |
| 0 | 20 155 (4531) | 20 155 (4531) | 18 754 (4216) | 17 824 (4007) | 17 824 (4007) | 15 115 (3398) | 13 998 (3147) | 13 438 (3021) | 7464 (1678) | 5413 (1217) |
| .2 | 18 847 (4237) | 19 034 (4279) | 17 450 (3923) | 16 423 (3692) | 16 049 (3608) | 14 372 (3231) | 13 625 (3063) | 12 504 (2811) | 7184 (1615) | 5133 (1154) |
| .4 | 17 170 (3860) | 18 665 (4196) | 15 862 (3566) | 14 555 (3272) | 14 741 (3314) | 13 438 (3021) | 13 345 (3000) | 11 570 (2601) | 6810 (1531) | 4853 (1091) |
| .6 | 15 302 (3440) | 18 478 (4154) | 14 555 (3272) | 13 158 (2958) | 13 812 (3105) | 12 130 (2727) | 13 158 (2958) | 10 636 (2391) | 6437 (1447) | 4573 (1028) |
| .8 | 13 438 (3021) | 18 291 (4112) | 13 812 (3105) | 11 757 (2643) | 12 878 (2895) | 10 822 (2433) | 12 971 (2916) | 9 706 (2182) | 6067 (1364) | 4293 ( 965) |
| 1.0 | 11 943 (2685) | 18 104 (4070) | 13 345 (3000) | 10 449 (2349) | 11 943 (2685) | 9 706 (2182) | 12 913 (2903) | 8 772 (1972) | 5694 (1280) | 4012 ( 902) |
| 1.2 | 10 822 (2433) | 17 917 (4028) | 12 971 (2916) | 9 332 (2098) | 11 383 (2559) | 8 959 (2014) | 12 878 (2895) | 8 025 (1804) | 5320 (1196) | 3732 ( 839) |
| 1.4 | 9 893 (2224) | | 12 691 (2853) | 8 398 (1888) | 10 822 (2433) | 8 211 (1846) | 12 784 (2874) | 7 277 (1636) | 5040 (1133) | 3545 ( 797) |
| 1.6 | 9 145 (2056) | | 12 504 (2811) | 7 838 (1762) | 10 449 (2349) | 7 464 (1678) | 12 726 (2861) | 6 717 (1510) | 4760 (1070) | 3358 ( 755) |
| 1.8 | 8 492 (1909) | | 12 410 (2790) | 7 090 (1594) | 10 080 (2266) | 6 904 (1552) | 12 691 (2853) | 6 161 (1385) | 4573 (1028) | 3078 ( 692) |
| 2.0 | 7 838 (1762) | | 11 917 (2679) | 6 530 (1468) | 9 706 (2182) | 6 437 (1447) | | 5 787 (1301) | 4293 ( 965) | 2891 ( 650) |
| 2.2 | 7 277 (1636) | | | 6 067 (1364) | 9 332 (2098) | 5 974 (1343) | | 5 413 (1217) | 4199 ( 944) | 2611 ( 587) |
| 2.4 | 6 904 (1552) | | | 5 600 (1259) | 9 145 (2056) | 5 600 (1259) | | 5 040 (1133) | 4106 ( 923) | 2424 ( 545) |
| 2.6 | 6 530 (1468) | | | 5 227 (1175) | 8 865 (1993) | 5 413 (1217) | | 4 666 (1049) | 4012 ( 902) | 2237 ( 503) |
| 2.8 | 6 161 (1385) | | | 4 853 (1091) | 8 585 (1930) | 5 040 (1133) | | 4 293 ( 965) | 3919 ( 881) | 2144 ( 482) |
| 3.0 | 5 787 (1301) | | | 4 479 (1007) | 8 398 (1888) | 4 760 (1070) | | 4 012 ( 902) | 3825 ( 860) | 1962 ( 441) |
| 3.2 | 5 413 (1217) | | | 4 293 ( 965) | 8 118 (1825) | 4 479 (1007) | | 3 732 ( 839) | 3732 ( 839) | 1868 ( 420) |
| 3.4 | 5 133 (1154) | | | 3 919 ( 881) | 7 838 (1762) | 4 293 ( 965) | | 3 452 ( 776) | | 1775 ( 399) |
| 3.6 | 4 853 (1091) | | | 3 732 ( 839) | 7 650 (1720) | 4 106 ( 923) | | 3 172 ( 713) | | 1681 ( 378) |
| 3.8 | 4 666 (1049) | | | 3 545 ( 797) | 7 557 (1699) | 3 919 ( 881) | | 2 985 ( 671) | | |
| 4.0 | 4 386 ( 986) | | | 3 265 ( 734) | 7 464 (1678) | 3 732 ( 839) | | 2 798 ( 629) | | |
| 4.2 | 4 106 ( 923) | | | 2 985 ( 671) | | | | 2 611 ( 587) | | |
| 4.4 | 3 919 ( 881) | | | 2 798 ( 629) | | | | 2 424 ( 545) | | |
| 4.6 | 3 732 ( 839) | | | 2 611 ( 587) | | | | 2 237 ( 503) | | |
| 4.8 | | | | 2 518 ( 566) | | | | 2 055 ( 462) | | |
| 5.0 | | | | 2 331 ( 524) | | | | 1 868 ( 420) | | |
| 5.2 | | | | 2 237 ( 503) | | | | 1 775 ( 399) | | |
| 5.4 | | | | 2 055 ( 462) | | | | 1 681 ( 378) | | |
| 5.6 | | | | 1 868 ( 420) | | | | | | |
| 5.8 | | | | 1 775 ( 399) | | | | | | |
| 6.0 | | | | 1 681 ( 378) | | | | | | |

## TABLE II.- MASS AND DIMENSIONAL CHARACTERISTICS OF SIMULATED AIRCRAFT

| | | |
|---|---|---|
| Weight, N (lbf) | 245 096 | (55 100) |
| Wing area, $m^2$ ($ft^2$) | 78 | (843) |
| Wing span, m (ft) | 24 | (78) |
| Mean aerodynamic chord, m (ft) | 3.58 | (11.74) |
| Center-of-gravity location, percent $\bar{c}$ | | 40 |
| $I_X$, kg-$m^2$ (slug-$ft^2$) | 331 103 | (244 212) |
| $I_Y$, kg-$m^2$ (slug-$ft^2$) | 334 637 | (246 819) |
| $I_Z$, kg-$m^2$ (slug-$ft^2$) | 625 677 | (461 482) |
| $I_{XZ}$, kg-$m^2$ (slug-$ft^2$) | 27 690 | (20 423) |
| Maximum control-surface deflections: | | |
| $\delta_t$, deg | | ±10 |
| $\delta_{f3}$, deg | | 0 to 90 |
| $\delta_{sp}$, deg | | 0 to 60 |
| $\delta_s$, deg | | ±60 |
| $\delta_a$, deg | | ±20 |
| $\delta_r$, deg | | ±40 |
| Maximum control-surface deflection rates: | | |
| $\dot{\delta}_t$, deg/sec | | 50 |
| $\dot{\delta}_{f3}$, deg/sec | | 5 |
| $\dot{\delta}_{sp}$, deg/sec | | 50 |
| $\dot{\delta}_s$, deg/sec | | 50 |
| $\dot{\delta}_a$, deg/sec | | 50 |
| $\dot{\delta}_r$, deg/sec | | 50 |

TABLE III.- BASIC AERODYNAMIC INPUTS USED IN SIMULATION

$\left[\delta_{\overline{f3}} = \delta_{f3} - 60\right]$

| $\alpha$, deg | $C_T$=0 | $C_T$=1.87 | $C_T$=3.74 | $C_T$=0 | $C_T$=1.87 | $C_T$=3.74 | $C_T$=0 | $C_T$=1.87 | $C_T$=3.74 | $C_T$=0 | $C_T$=1.87 | $C_T$=3.74 | $C_T$=0 | $C_T$=1.87 | $C_T$=3.74 | $C_T$=0 | $C_T$=1.87 | $C_T$=3.74 | $C_T$=0 | $C_T$=1.87 | $C_T$=3.74 | $C_T$=0 | $C_T$=1.87 | $C_T$=3.74 |
|---|---|---|---|---|---|---|---|---|---|---|---|---|---|---|---|---|---|---|---|---|---|---|---|---|
| | $C_X$ | | | $C_Z$ | | | $C_m$ | | | $C_{X_{\delta_{\overline{f3}}}}$, per deg | | | $C_{Z_{\delta_{\overline{f3}}}}$, per deg | | | $C_{m_{\delta_{\overline{f3}}}}$, per deg | | | $C_{m_q}$, per rad | | | $C_{m_{\dot{\alpha}}}$, per rad | | |
| -10 | -0.330 | -0.211 | 0.383 | -0.145 | -3.212 | -4.739 | 0.80 | 0.25 | -0.50 | -0.0038 | -0.0460 | -0.0760 | -0.0180 | -0.0550 | -0.0400 | -0.0001 | 0.0016 | -0.0036 | -28.60 | -17.86 | -28.60 | -11.40 | -7.14 | -11.40 |
| -5 | -.366 | -.232 | .285 | -.741 | -3.794 | -5.345 | .45 | .10 | -.50 | -.0033 | -.0435 | -.0736 | -.0134 | -.0580 | -.0610 | .0006 | .0021 | -.0023 | -28.60 | -26.80 | -28.60 | -11.40 | -10.70 | -11.40 |
| 0 | -.340 | -.250 | .300 | -1.400 | -4.500 | -6.130 | .12 | -.07 | -.53 | -.0026 | -.0403 | -.0700 | -.0086 | -.0611 | -.0861 | .0013 | .0026 | -.0010 | -28.60 | -32.15 | -29.30 | -11.40 | -12.85 | -11.70 |
| 5 | -.249 | -.119 | .432 | -2.090 | -5.180 | -6.889 | -.14 | -.25 | -.60 | -.0029 | -.0388 | -.0690 | -.0089 | -.0593 | -.0832 | .0019 | .0022 | 0 | -26.45 | -34.30 | -30.00 | -10.55 | -13.70 | -12.00 |
| 10 | -.094 | .095 | .594 | -2.518 | -5.781 | -7.572 | -.23 | -.37 | -.68 | -.0040 | -.0371 | -.0674 | -.0040 | -.0534 | -.0784 | .0019 | .0034 | .0003 | -21.44 | -32.86 | -30.36 | -8.56 | -13.14 | -12.14 |
| 15 | .017 | .344 | .932 | -2.770 | -6.306 | -8.116 | -.27 | -.45 | -.78 | -.0041 | -.0360 | -.0649 | .0009 | -.0490 | -.0759 | .0033 | .0030 | .0005 | -10.72 | -30.72 | -31.45 | -4.28 | -12.28 | -12.55 |
| 20 | .019 | .632 | 1.162 | -2.851 | -6.708 | -8.601 | -.27 | -.50 | -.84 | -.0051 | -.0350 | -.0627 | .0054 | -.0492 | -.0737 | .0026 | .0020 | -.0005 | -3.57 | -30.00 | -31.45 | -1.43 | -12.00 | -12.55 |
| 25 | .078 | .864 | 1.535 | -2.700 | -7.033 | -8.972 | -.30 | -.49 | -.83 | -.0046 | -.0320 | -.0591 | .0040 | -.0455 | -.0734 | .0030 | .0016 | -.0004 | -5.00 | -28.60 | -30.36 | -2.00 | -11.40 | -12.14 |
| 30 | .111 | .798 | 1.765 | -2.592 | -5.602 | -9.258 | -.32 | -.40 | -.75 | -.0055 | -.0099 | -.0514 | .0060 | -.0527 | -.0683 | .0022 | .0042 | -.0006 | -9.29 | -39.30 | -48.60 | -3.71 | -15.70 | -19.40 |
| | $C_{X_{\delta_s}}$, per deg | | | $C_{Z_{\delta_s}}$, per deg | | | $C_{m_{\delta_s}}$, per deg | | | $C_{Y_{\delta_s}}$, per deg | | | $C_{n_{\delta_s}}$, per deg | | | $C_{l_{\delta_s}}$, per deg | | | $C_{Y_p}$, per rad | | | $C_{n_p}$, per rad | | |
| -10 | -0.0012 | -0.0024 | -0.0026 | 0.0093 | 0.0140 | 0.0148 | -0.0012 | 0.0006 | 0.0052 | -0.0002 | 0 | 0.0002 | 0.0007 | 0.0007 | 0.0005 | 0.0015 | 0.0023 | 0.0024 | -0.02 | -0.09 | -0.49 | -0.15 | -0.11 | 0.38 |
| -5 | -.0016 | -.0016 | -.0028 | .0105 | .0165 | .0161 | -.0017 | -.0007 | .0025 | -.0002 | -.0001 | .0002 | .0008 | .0008 | .0009 | .0020 | .0029 | .0028 | -.04 | -.04 | -.10 | -.04 | -.15 | -.12 |
| 0 | -.0020 | -.0008 | -.0030 | .0117 | .0192 | .0173 | -.0022 | -.0020 | -.0002 | -.0002 | -.0002 | 0 | .0009 | .0009 | .0013 | .0025 | .0035 | .0032 | 0 | .05 | .11 | -.02 | -.22 | -.30 |
| 5 | -.0026 | -.0013 | -.0032 | .0128 | .0209 | .0173 | -.0008 | -.0022 | -.0017 | -.0002 | -.0002 | -.0001 | .0009 | .0010 | .0015 | .0027 | .0038 | .0033 | .07 | .19 | .10 | -.20 | -.28 | -.25 |
| 10 | -.0033 | -.0021 | -.0028 | .0119 | .0217 | .0185 | -.0002 | -.0020 | -.0020 | -.0003 | -.0003 | -.0002 | .0009 | .0011 | .0015 | .0026 | .0038 | .0032 | .05 | .25 | .53 | -.16 | -.33 | -.40 |
| 15 | -.0035 | -.0033 | -.0046 | .0099 | .0219 | .0186 | .0008 | -.0012 | -.0012 | -.0002 | -.0003 | -.0002 | .0009 | .0011 | .0015 | .0022 | .0036 | .0031 | .24 | .45 | .80 | -.20 | -.45 | -.52 |
| 20 | -.0028 | -.0037 | -.0033 | .0078 | .0210 | .0176 | .0013 | -.0008 | -.0005 | -.0002 | -.0003 | -.0002 | .0008 | .0011 | .0014 | .0017 | .0035 | .0029 | .30 | .80 | 1.20 | -.22 | -.50 | -.57 |
| 25 | -.0017 | -.0032 | -.0048 | .0036 | .0209 | .0163 | .0017 | -.0008 | -.0002 | -.0002 | -.0004 | -.0002 | .0008 | .0010 | .0013 | .0011 | .0037 | .0028 | .06 | .89 | 1.25 | -.15 | -.40 | -.59 |
| 30 | 0 | -.0068 | -.0029 | .0015 | .0117 | .0160 | .0020 | -.0012 | -.0005 | -.0002 | -.0004 | -.0003 | .0007 | .0010 | .0012 | .0008 | .0038 | .0028 | .13 | .75 | 1.03 | -.14 | -.22 | -.15 |
| | $C_{X_{\delta_t}}$, per deg | | | $C_{Z_{\delta_t}}$, per deg | | | $C_{m_{\delta_t}}$, per deg | | | $C_{Y_{\delta_r}}$, per deg | | | $C_{n_{\delta_r}}$, per deg | | | $C_{l_{\delta_r}}$, per deg | | | $C_{l_p}$, per rad | | | $C_{Y_r}$, per rad | | |
| -10 | -0.0092 | 0.0072 | -0.0049 | -0.0242 | -0.0160 | -0.0102 | -0.090 | -0.084 | -0.028 | 0.012 | 0.010 | 0.009 | -0.0043 | -0.0051 | -0.0046 | 0.0020 | 0.0016 | 0.0019 | -0.05 | -1.13 | -0.78 | 0.76 | 0.88 | 0.94 |
| -5 | -.0062 | .0042 | -.0019 | -.0246 | -.0204 | -.0101 | -.085 | -.087 | -.044 | .012 | .010 | .009 | -.0041 | -.0047 | -.0046 | .0018 | .0016 | .0020 | -.60 | -.88 | -.75 | .76 | .86 | .92 |
| 0 | -.0030 | .0010 | .0010 | -.0250 | -.0250 | -.0100 | -.080 | -.090 | -.060 | .012 | .010 | .009 | -.0039 | -.0043 | -.0046 | .0016 | .0016 | .0021 | -.98 | -.68 | -.72 | .77 | .90 | 1.00 |
| 5 | -.0002 | -.0012 | .0004 | -.0201 | -.0202 | -.0050 | -.065 | -.097 | -.076 | .011 | .010 | .009 | -.0038 | -.0041 | -.0046 | .0016 | .0017 | .0022 | -.68 | -.50 | -.68 | .77 | 1.03 | 1.20 |
| 10 | -.0036 | -.0044 | -.0070 | -.0138 | -.0211 | -.0174 | -.040 | -.092 | -.088 | .010 | .010 | .009 | -.0036 | -.0040 | -.0046 | .0016 | .0017 | .0022 | -.40 | -.50 | -.63 | .78 | 1.08 | 1.60 |
| 15 | -.0018 | -.0071 | -.0015 | -.0088 | -.0122 | -.0252 | -.013 | -.078 | -.098 | .010 | .010 | .010 | -.0034 | -.0040 | -.0046 | .0011 | .0017 | .0022 | -.37 | -.50 | -.55 | .80 | 1.00 | 1.35 |
| 20 | -.0006 | -.0011 | .0002 | -.0042 | -.0057 | -.0180 | .002 | -.069 | -.089 | .009 | .011 | .010 | -.0024 | -.0040 | -.0046 | .0003 | .0016 | .0020 | -.32 | -.33 | -.42 | .59 | .70 | 1.24 |
| 25 | -.0042 | -.0051 | -.0030 | -.0053 | -.0079 | -.0124 | .002 | -.060 | -.080 | .006 | .012 | .012 | -.0020 | -.0041 | -.0047 | -.0003 | .0010 | .0017 | -.26 | -.17 | -.33 | .33 | .32 | .93 |
| 30 | -.0002 | -.0152 | .0339 | -.0036 | -.0312 | -.0728 | -.005 | -.050 | -.079 | .002 | .010 | .012 | -.0002 | -.0033 | -.0042 | .0006 | .0008 | .0014 | -.26 | -.08 | -.25 | -.08 | 1.70 | 2.55 |
| | $C_{Y_\beta}$, per deg | | | $C_{n_\beta}$, per deg | | | $C_{l_\beta}$, per deg | | | $C_{X_{\delta_{sp}}}$, per deg | | | $C_{Z_{\delta_{sp}}}$, per deg | | | $C_{m_{\delta_{sp}}}$, per deg | | | $C_{n_r}$, per rad | | | $C_{l_r}$, per rad | | |
| -10 | -0.020 | -0.022 | -0.050 | 0.0030 | 0.0035 | 0.0053 | 0.0012 | 0 | 0 | 0 | -0.0060 | -0.0044 | 0.0260 | 0.0430 | 0.0300 | -0.006 | 0 | 0.008 | -0.45 | -0.33 | -0.37 | 0.32 | 0.57 | 0.55 |
| -5 | -.020 | -.050 | -.050 | .0038 | .0052 | .0070 | -.0006 | -.0020 | -.0020 | -.0016 | -.0043 | -.0042 | .0272 | .0425 | .0325 | -.004 | 0 | .005 | -.35 | -.38 | -.42 | .48 | .70 | .77 |
| 0 | -.020 | -.050 | -.055 | .0042 | .0078 | .0081 | -.0024 | -.0036 | -.0031 | -.0040 | -.0010 | -.0040 | .0290 | .0420 | .0380 | -.002 | 0 | .002 | -.30 | -.42 | -.45 | .67 | .80 | .86 |
| 5 | -.020 | -.050 | -.055 | .0043 | .0082 | .0086 | -.0034 | -.0048 | -.0044 | -.0048 | -.0018 | -.0056 | .0317 | .0440 | .0417 | 0 | 0 | .001 | -.33 | -.41 | -.45 | .77 | .85 | .85 |
| 10 | -.020 | -.050 | -.055 | .0043 | .0080 | .0081 | -.0023 | -.0051 | -.0053 | -.0052 | -.0016 | -.0045 | .0296 | .0434 | .0429 | .001 | 0 | .001 | -.34 | -.42 | -.54 | .83 | .80 | .80 |
| 15 | -.023 | -.050 | -.055 | .0047 | .0082 | .0089 | -.0028 | -.0051 | -.0061 | -.0046 | -.0012 | -.0080 | .0247 | .0432 | .0414 | .004 | .001 | .002 | -.38 | -.42 | -.52 | .88 | .82 | .83 |
| 20 | -.024 | -.050 | -.055 | .0050 | .0084 | .0092 | -.0029 | -.0062 | -.0066 | -.0036 | -.0046 | -.0070 | .0157 | .0420 | .0387 | .005 | .001 | .002 | -.35 | -.40 | -.52 | .73 | .90 | .90 |
| 25 | -.020 | -.050 | -.055 | .0021 | .0083 | .0088 | -.0070 | -.0067 | -.0072 | .0001 | -.0025 | -.0085 | .0045 | .0408 | .0347 | .004 | .001 | .003 | -.30 | -.34 | -.47 | .83 | 1.10 | .93 |
| 30 | -.024 | -.020 | -.055 | .0018 | -.0040 | .0082 | -.0050 | -.0070 | -.0090 | .0012 | -.0082 | -.0024 | .0019 | -.0022 | .0321 | .004 | .001 | .003 | -.20 | -.42 | -.70 | .62 | -.20 | -.50 |

TABLE III.- BASIC AERODYNAMIC INPUTS USED IN SIMULATION – Concluded

| $\alpha$, deg | $C_T$=0 | $C_T$=0.70 | $C_T$=1.40 | $C_T$=2.10 | $C_T$=2.81 | $C_T$=0 | $C_T$=0.70 | $C_T$=1.40 | $C_T$=2.10 | $C_T$=2.81 | $C_T$=0 | $C_T$=0.70 | $C_T$=1.40 | $C_T$=2.10 | $C_T$=2.81 |
|---|---|---|---|---|---|---|---|---|---|---|---|---|---|---|---|
| | $C_{Y_{\delta_a}}$, per deg | | | | | $C_{n_{\delta_a}}$, per deg | | | | | $C_{l_{\delta_a}}$, per deg | | | | |
| -10 | -0.0016 | -0.0010 | -0.0004 | 0.0002 | 0.0008 | -0.0014 | -0.0028 | -0.0040 | -0.0052 | -0.0064 | 0.0082 | 0.0083 | 0.0084 | 0.0085 | 0.0086 |
| -5 | -.0012 | -.0007 | -.0002 | .0003 | .0008 | -.0001 | -.0017 | -.0032 | -.0047 | -.0062 | .0048 | .0058 | .0068 | .0078 | .0088 |
| 0 | -.0008 | -.0004 | 0 | .0004 | .0008 | .0012 | -.0006 | -.0024 | -.0042 | -.0060 | .0014 | .0033 | .0052 | .0071 | .0090 |
| 5 | -.0004 | -.0002 | 0 | .0002 | .0004 | -.0010 | -.0022 | -.0034 | -.0046 | -.0058 | .0014 | .0033 | .0052 | .0071 | .0090 |
| 10 | -.0006 | -.0004 | -.0002 | 0 | .0002 | -.0010 | -.0022 | -.0034 | -.0046 | -.0058 | .0010 | .0030 | .0050 | .0070 | .0090 |
| 15 | -.0008 | -.0006 | -.0004 | -.0002 | .0001 | .0004 | -.0011 | -.0026 | -.0041 | -.0056 | .0027 | .0044 | .0061 | .0078 | .0096 |
| 20 | -.0022 | -.0018 | -.0014 | -.0010 | -.0005 | .0045 | .0026 | .0007 | -.0012 | -.0032 | .0207 | .0197 | .0187 | .0177 | .0168 |
| 25 | -.0036 | -.0024 | -.0012 | 0 | -.0012 | .0036 | .0024 | .0010 | -.0002 | -.0014 | -.0010 | .0050 | .0110 | .0170 | .0240 |
| 30 | -.0007 | -.0006 | -.0005 | -.0004 | -.0003 | .0024 | .0008 | -.0008 | -.0024 | -.0040 | -.0076 | -.0012 | .0052 | .0116 | .0180 |

TABLE IV.- SIMULATOR CONTROL CHARACTERISTICS

| Control | Maximum travel in – | | | Breakout force | | Force gradient | |
|---|---|---|---|---|---|---|---|
| | deg | cm | in. | N | lbf | N/cm | lbf/in. |
| Column: | | | | | | | |
| Forward | 9.9 | 13.97 | 5.50 | 13.3 | 3.0 | 14.0 | 8.0 |
| Aft | 20.5 | 25.25 | 9.94 | | | | |
| Wheel | ±130.0 | ±37.34 | ±14.70 | 11.1 | 2.5 | 5.3 | 3.0 |
| Pedal | | 10.80 | 4.25 | 31.1 | 7.0 | 28.9 | 16.5 |

TABLE V.- PILOT RATING SYSTEM

| | | | | |
|---|---|---|---|---|
| CONTROLLABLE<br>Capable of being controlled or managed in context of mission, with available pilot attention. | ACCEPTABLE<br>May have deficiencies which warrant improvement, but adequate for mission.<br>Pilot compensation, if required to achieve acceptable performance, is feasible. | SATISFACTORY<br>Meets all requirements and expectations; good enough without improvement.<br>Clearly adequate for mission. | Excellent, highly desirable. | 1 |
| | | | Good, pleasant, well behaved. | 2 |
| | | | Fair. Some mildly unpleasant characteristics. Good enough for mission without improvement. | 3 |
| | | UNSATISFACTORY<br>Reluctantly acceptable. Deficiencies which warrant improvement. Performance adequate for mission with feasible pilot compensation. | Some minor but annoying deficiencies. Improvement is requested. Effect on performance is easily compensated for by pilot. | 4 |
| | | | Moderately objectionable deficiencies. Improvement is needed. Reasonable performance requires considerable pilot compensation. | 5 |
| | | | Very objectionable deficiencies. Major improvements are needed. Requires best available pilot compensation to achieve acceptable performance. | 6 |
| | UNACCEPTABLE<br>Deficiencies which require improvement. Inadequate performance for mission even with maximum feasible pilot compensation. | | Major deficiencies which require improvement for acceptance. Controllable. Performance inadequate for mission, or pilot compensation required for minimum acceptable performance in mission is too high. | 7 |
| | | | Controllable with difficulty. Requires substantial pilot skill and attention to retain control and continue mission. | 8 |
| | | | Marginally controllable in mission. Requires maximum available pilot skill and attention to retain control. | 9 |
| UNCONTROLLABLE<br>Control will be lost during some portion of mission. | | | Uncontrollable in mission. | 10 |

TABLE VI.- PREFILTER G AND FEEDBACK F GAIN MATRICES FOR THE DECOUPLED LONGITUDINAL CONTROLLER MECHANIZATION THAT USED THROTTLE, HORIZONTAL TAIL, AND FLAPS AS ACTIVE CONTROL ELEMENTS

$\omega_{sp} = 9.213$ rad/sec

$\zeta_{sp} = 0.71$

$P_{sp} = 0.97$ sec

$\left(t_{1/2}\right)_{sp} = 0.11$ sec

$$G = \begin{bmatrix} 3.836472 & -3.179248 & -0.779137 \\ 0.229078 & -0.743277 & -22.100632 \\ 3.096225 & -12.985945 & 11.447270 \end{bmatrix}$$

$$F = \begin{bmatrix} 0.003958 & 0.009820 & 0.003333 & 0.047180 \\ -21.871555 & -31.805814 & 0.115047 & -0.607917 \\ 14.543495 & 18.720207 & -1.086099 & -9.307316 \end{bmatrix}$$

TABLE VII.- PREFILTER G AND FEEDBACK F GAIN MATRICES FOR THE DECOUPLED LONGITUDINAL CONTROLLER MECHANIZATION THAT USED HORIZONTAL TAIL, FLAPS, AND SYMMETRIC SPOILERS AS ACTIVE CONTROL ELEMENTS

| | |
|---|---|
| $\omega_{sp} = 6.130$ rad/sec | $\omega_{ph} = 0.782$ rad/sec |
| $\zeta_{sp} = 0.71$ | $\zeta_{ph} = 0.84$ |
| $P_{sp} = 1.46$ sec | $P_{ph} = 14.69$ sec |
| $\left(t_{1/2}\right)_{sp}$ | $\left(t_{1/2}\right)_{ph} = 1.06$ sec |

$$G = \begin{bmatrix} 0.100700 & -0.025717 & -10.123130 \\ -0.769160 & -3.180786 & -0.614765 \\ -5.847425 & 4.468931 & -1.291020 \end{bmatrix}$$

$$F = \begin{bmatrix} -9.928536 & -20.359053 & 0.125552 & 0.010427 \\ 1.155006 & 1.562071 & -0.408029 & -2.184983 \\ -3.968101 & -5.288998 & 1.867448 & 1.118906 \end{bmatrix}$$

TABLE VIII.- COMPARISON OF SINK RATE AND TOUCHDOWN POINT ATTAINED USING CONVENTIONAL CONTROLS WITH SAS WITH THOSE ATTAINED USING DECOUPLED LONGITUDINAL CONTROLS AND CONVENTIONAL LATERAL CONTROLS

[Zero x denotes runway threshold]

| Controls | $\mu_{\dot{h}}$, m/sec (ft/sec) | $\sigma_{\dot{h}}$, m/sec (ft/sec) | $\mu_x$, meters (ft) | $\sigma_x$, meters (ft) | No. of runs | No. of runs outside desired landing area | |
|---|---|---|---|---|---|---|---|
| | | | | | | Short | Long |
| Two-segment approaches | | | | | | | |
| Conventional with SAS, $0 \leqq \sigma_W \leqq 1.22$ m/sec (4 ft/sec) | 2.38 (7.8) | 1.25 (4.1) | 143.6 (471.0) | 91.1 (299.1) | 23 | 5 | 3 |
| Decoupled longitudinal, $\sigma_W < 0.61$ m/sec (2 ft/sec) | 1.50 (4.9) | 0.70 (2.3) | 131.3 (430.8) | 48.0 (157.5) | 33 | 3 | 2 |
| Decoupled longitudinal, $\sigma_W \geqq 0.61$ m/sec (2 ft/sec) | 1.59 (5.2) | 1.02 (3.4) | 146.3 (479.9) | 87.0 (285.5) | 25 | 3 | 5 |
| $6^{\circ}$ approaches | | | | | | | |
| Decoupled longitudinal, $\sigma_W < 0.61$ m/sec (2 ft/sec) | 1.60 (5.2) | 0.79 (2.6) | 168.5 (552.8) | 68.9 (226.1) | 36 | 1 | 9 |
| Decoupled longitudinal, $\sigma_W \geqq 0.61$ m/sec (2 ft/sec) | 1.75 (5.7) | 0.89 (2.9) | 186.7 (612.7) | 71.7 (235.1) | 61 | 2 | 21 |

TABLE IX.- PREFILTER G AND FEEDBACK F GAIN MATRICES FOR DECOUPLED LATERAL CONTROL

$\omega_R = 2.298$ rad/sec

$\zeta_R = 0.80$

$P_R = 4.54$ sec

$\left(t_{1/2}\right)_R = 0.38$ sec

$$G = \begin{bmatrix} -7.734535 & 1.588237 & 0.0 \\ 6.267414 & 0.714128 & 0.0 \\ 13.962874 & -1.067195 & 0.0 \end{bmatrix}$$

$$F = \begin{bmatrix} 0.868495 & 6.990785 & -21.222495 & 0.122524 \\ 0.273273 & 2.615730 & -2.238758 & -0.116009 \\ -0.374135 & -1.615966 & 33.748233 & -0.522822 \end{bmatrix}$$

TABLE X.- SUMMARY OF SINK RATE AND TOUCHDOWN POINT ATTAINED USING DECOUPLED LONGITUDINAL AND LATERAL CONTROLS

[Zero x denotes runway threshold]

| Wind condition | $\mu_{\dot{h}}$, m/sec (ft/sec) | $\sigma_{\dot{h}}$, m/sec (ft/sec) | $\mu_x$, meters (ft) | $\sigma_x$, meters (ft) | No. of runs | No. of runs outside desired landing area | |
|---|---|---|---|---|---|---|---|
| | | | | | | Short | Long |
| $\sigma_w < 0.61$ m/sec (2 ft/sec) | 0.94 (3.1) | 0.67 (2.2) | 176.7 (579.9) | 64.8 (212.6) | 51 | 3 | 8 |
| $\sigma_w \geqq 0.61$ m/sec (2 ft/sec) | 1.00 (3.3) | 0.74 (2.4) | 173.2 (568.4) | 83.6 (274.3) | 47 | 2 | 13 |
| Crosswinds $\leqq$ 3.05 m/sec (10 ft/sec) | 0.81 (2.6) | 0.53 (1.7) | 162.7 (533.9) | 73.4 (241.0) | 47 | 2 | 11 |
| Crosswinds > 3.05 m/sec (10 ft/sec) | 1.11 (3.6) | 0.76 (2.5) | 183.1 (600.9) | 69.8 (229.1) | 66 | 1 | 18 |

TABLE XI.- PREFILTER G AND FEEDBACK F GAIN MATRICES FOR THE DECOUPLED LONGITUDINAL CONTROL MECHANIZATION THAT EMPLOYED THROTTLE, HORIZONTAL TAIL, FLAPS, AND SYMMETRIC SPOILERS AS ACTIVE CONTROL ELEMENTS

$\omega_{sp} = 5.36$ rad/sec

$\zeta_{sp} = 0.79$

$P_{sp} = 1.93$ sec

$\left(t_{1/2}\right)_{sp} = 0.16$ sec

$$G = \begin{bmatrix} 1.479356 & 3.424809 & 0.882762 & 0.0 \\ 2.638624 & 0.319423 & -7.582873 & 0.0 \\ 12.143196 & -4.229370 & -8.572163 & 0.0 \\ -11.227652 & 0.079126 & 6.239296 & 0.0 \end{bmatrix}$$

$$F = \begin{bmatrix} 1.615774 & -0.397886 & -2.006868 & 3.845354 \\ -4.873305 & -16.546972 & -2.428593 & 0.368500 \\ 5.489366 & -0.247396 & -13.759019 & -2.883877 \\ -2.592946 & 2.912773 & 6.699955 & -2.834244 \end{bmatrix}$$

TABLE XII.- SUMMARY OF SINK RATE AND TOUCHDOWN POINTS USING DECOUPLED LONGITUDINAL AND LATERAL CONTROLS FOR DECELERATING APPROACHES

[Zero x denotes runway threshold]

| Turbulence level | $\mu_{\dot{h}}$, m/sec (ft/sec) | $\sigma_{\dot{h}}$, m/sec (ft/sec) | $\mu_x$, meters (ft) | $\sigma_x$, meters (ft) | No. of runs | No. of runs outside desired landing area | |
|---|---|---|---|---|---|---|---|
| | | | | | | Short | Long |
| $\sigma_W < 0.61$ m/sec (2 ft/sec) | 1.18 (3.9) | 0.56 (1.8) | 156.5 (513.6) | 61.8 (202.7) | 42 | 0 | 10 |
| $\sigma_W \geqq 0.61$ m/sec (2 ft/sec) | 1.34 (4.4) | 0.62 (2.0) | 147.4 (483.5) | 57.8 (189.7) | 31 | 2 | 7 |

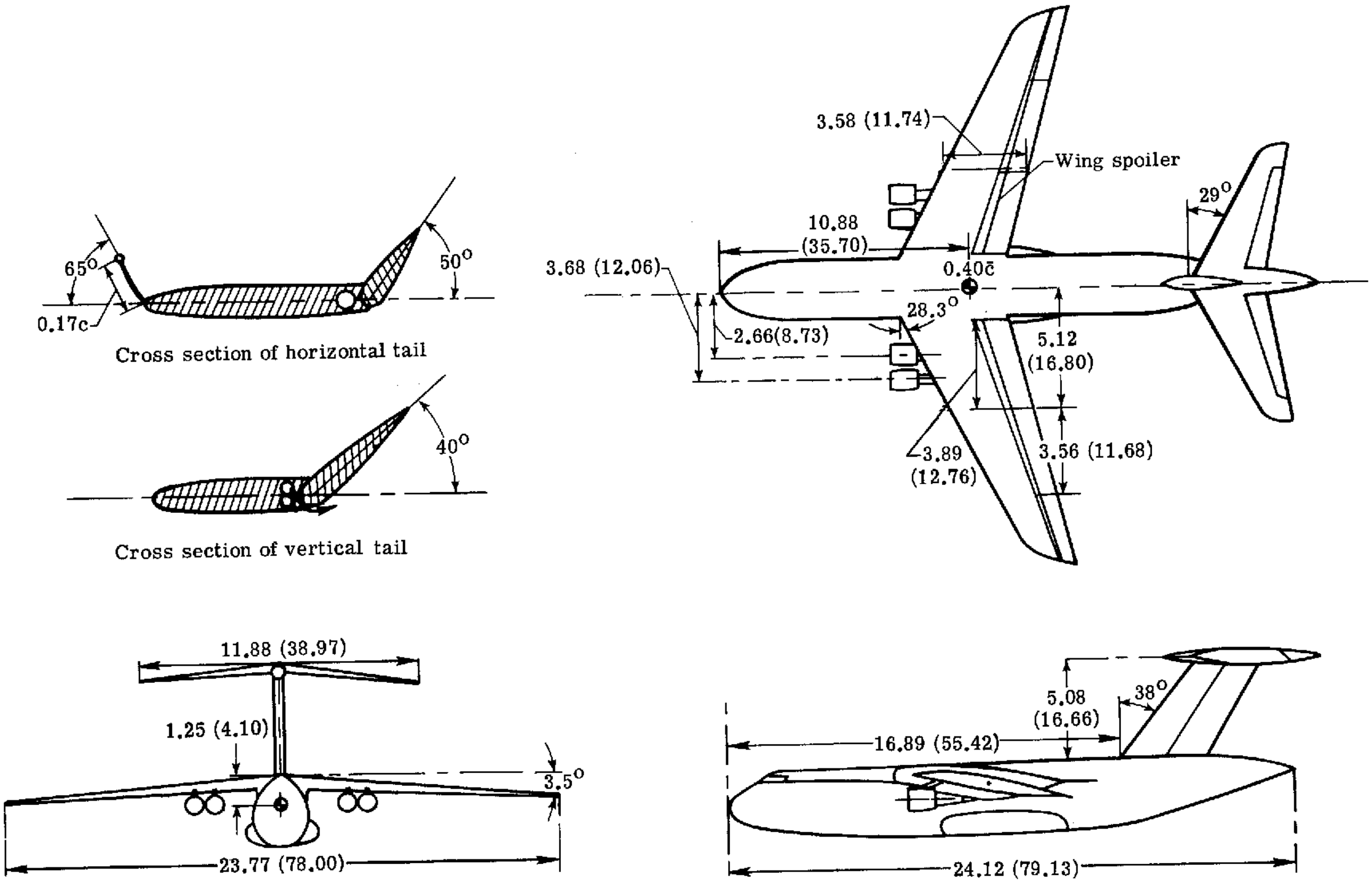


Figure 1.- Three-view drawing of simulated airplane. (All linear dimensions are in meters (ft).)

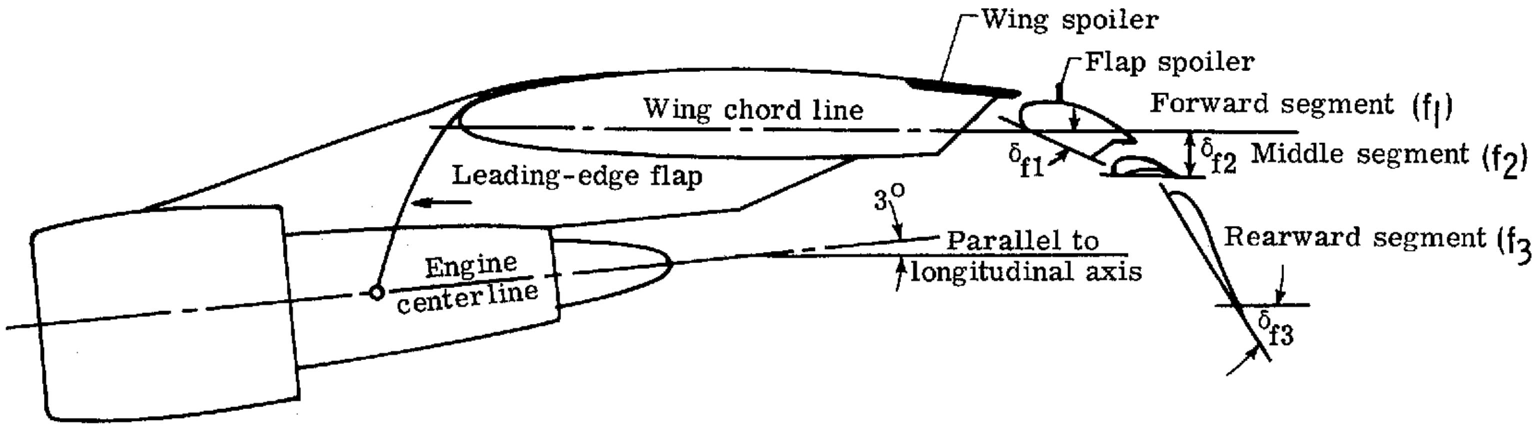


Figure 2.- Flap assembly and engine pylon detail. $\delta_{f1} = 25^{\circ}$; $\delta_{f2} = 10^{\circ}$; $\delta_{f3} = 60^{\circ}$.

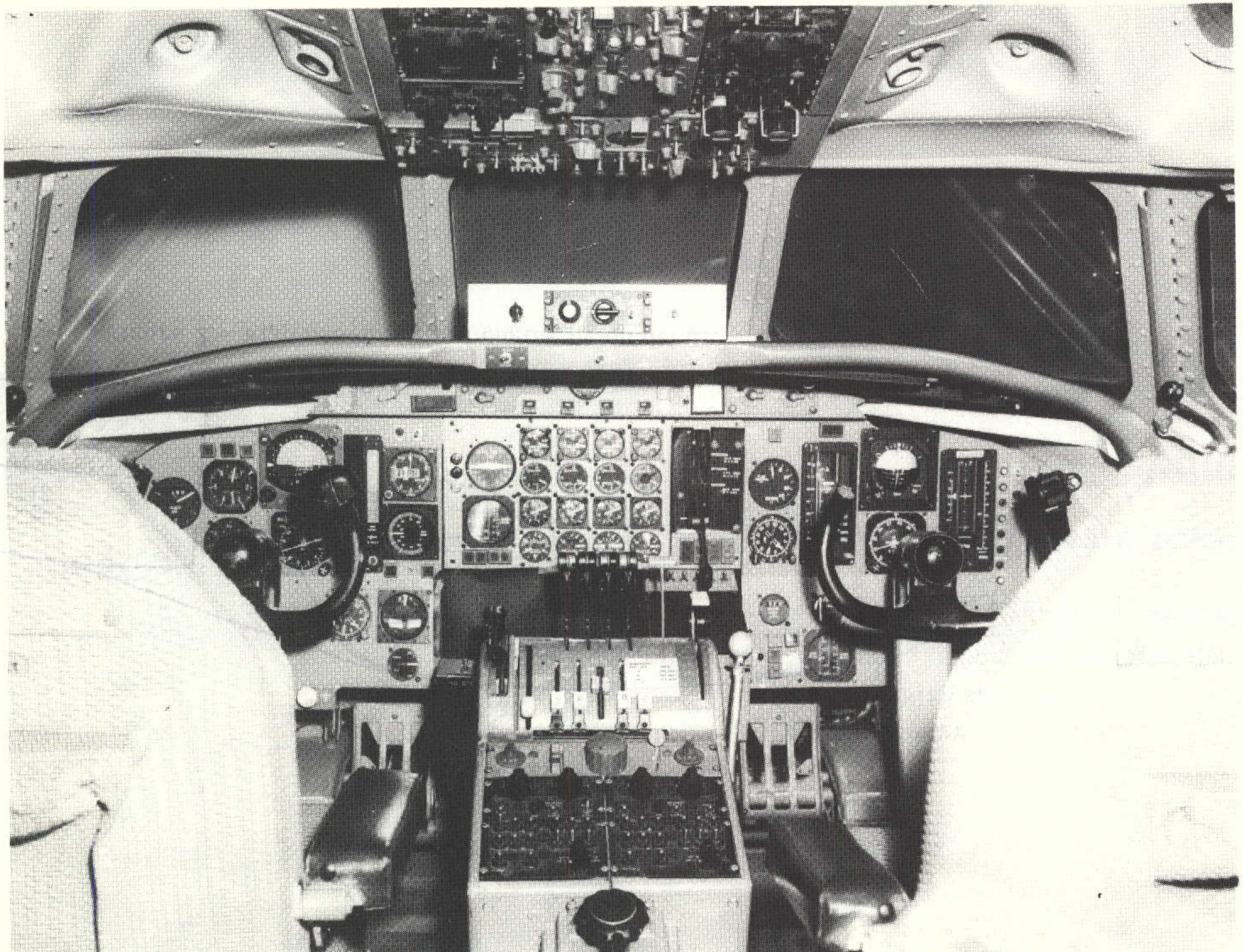

L-69-4142

Figure 3.- Simulator cockpit.

L-71-4272

Figure 4.- Photograph of $\frac{1}{300}$-scale airport model.

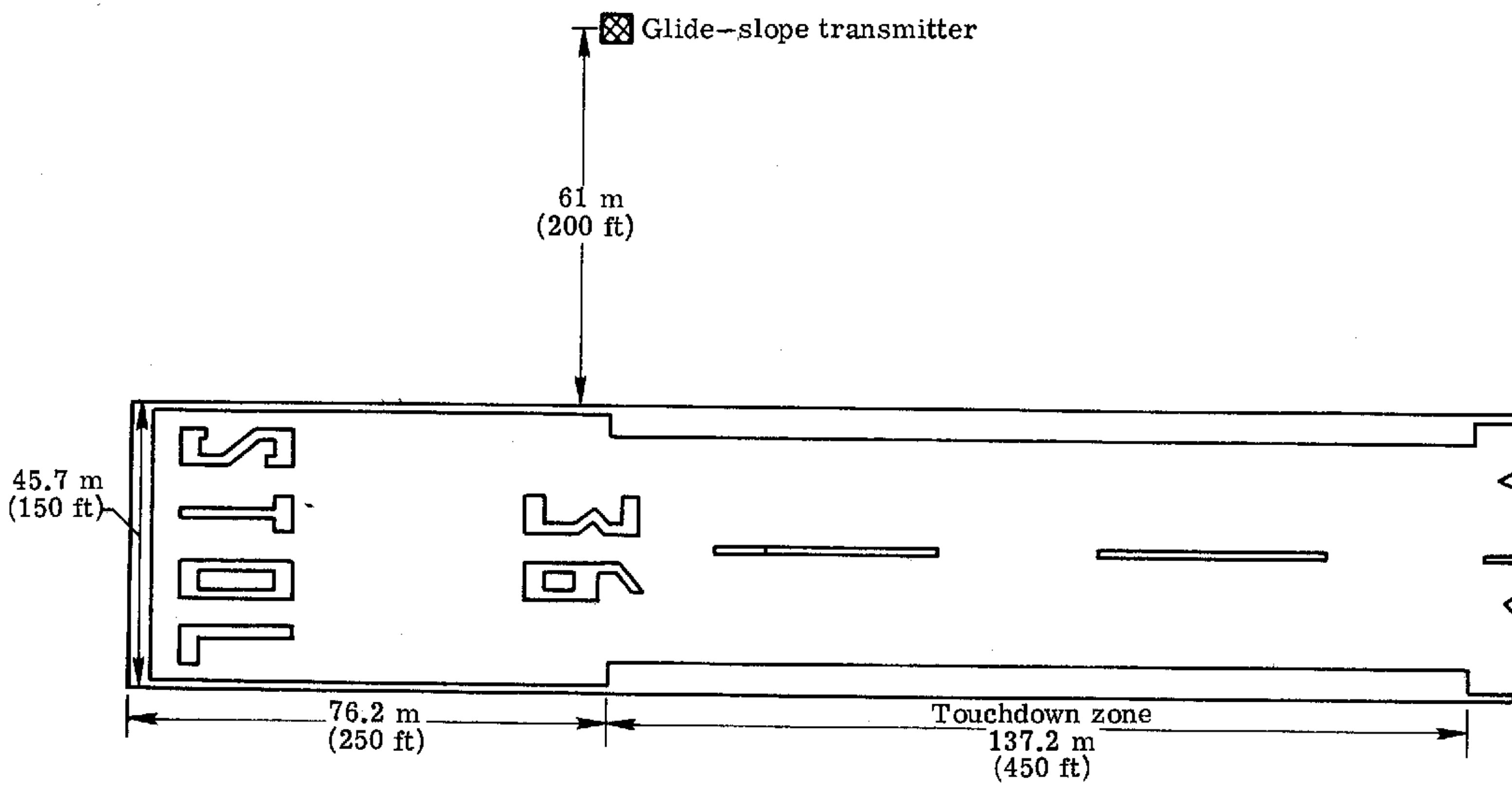


Figure 5.- Sketch of approach end of simulated runway.

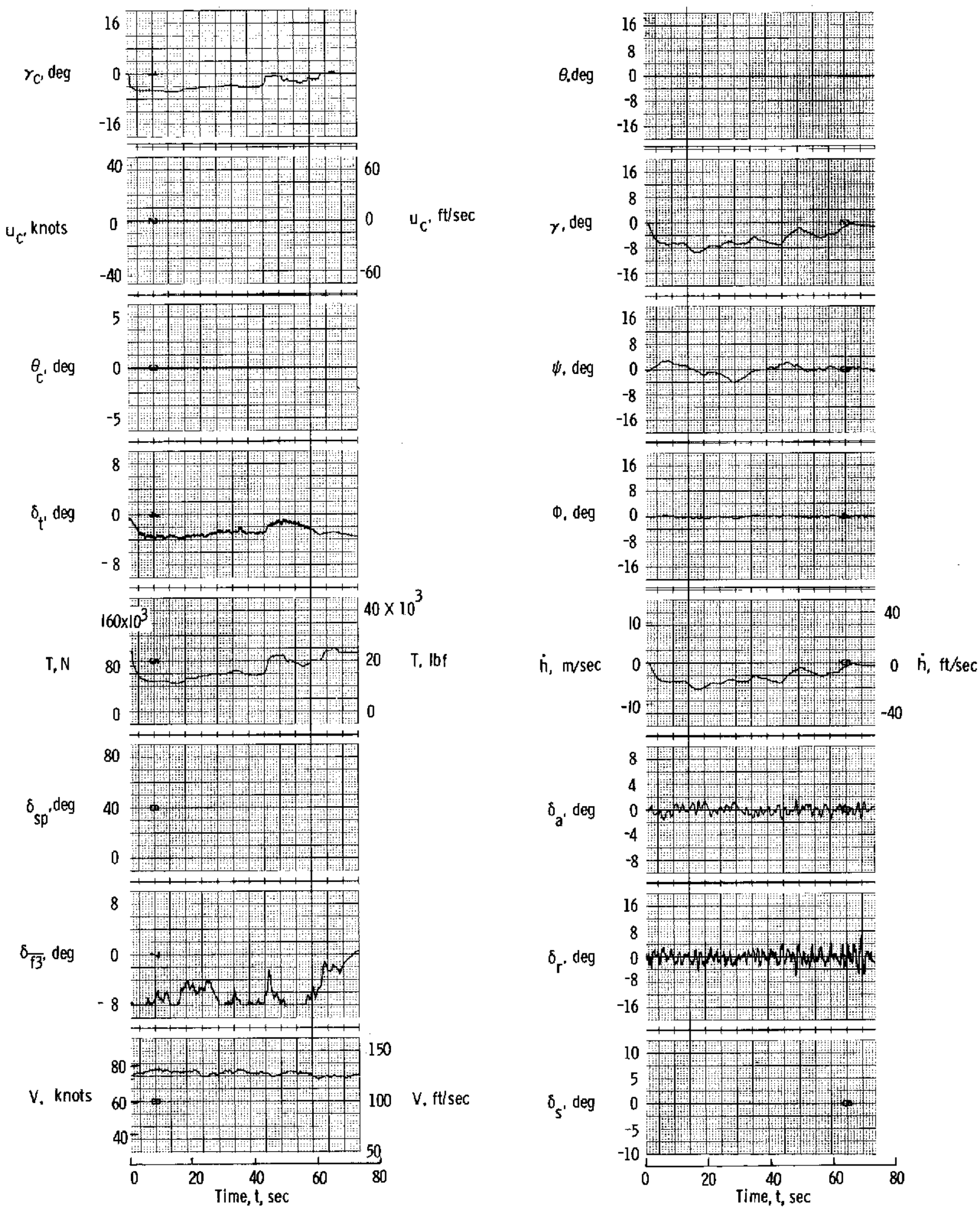


Figure 6.- Constant-speed approach using throttle, horizontal tail, and flaps to provide decoupled longitudinal control in turbulence with $\sigma_w = 0.61$ m/sec (2 ft/sec).

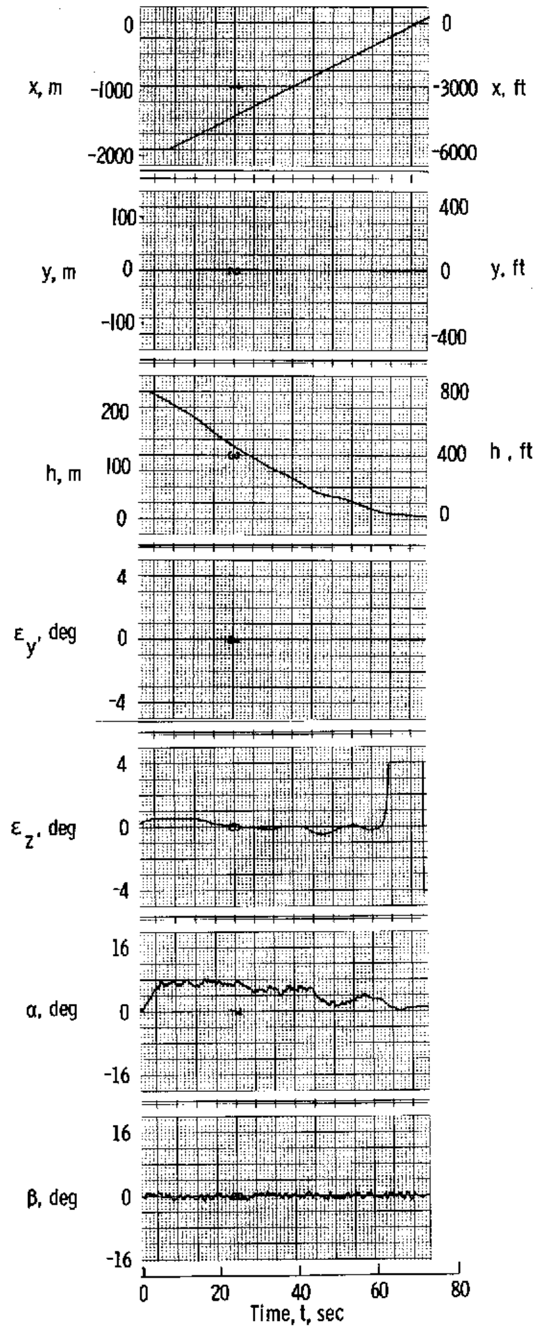


Figure 6.- Concluded.

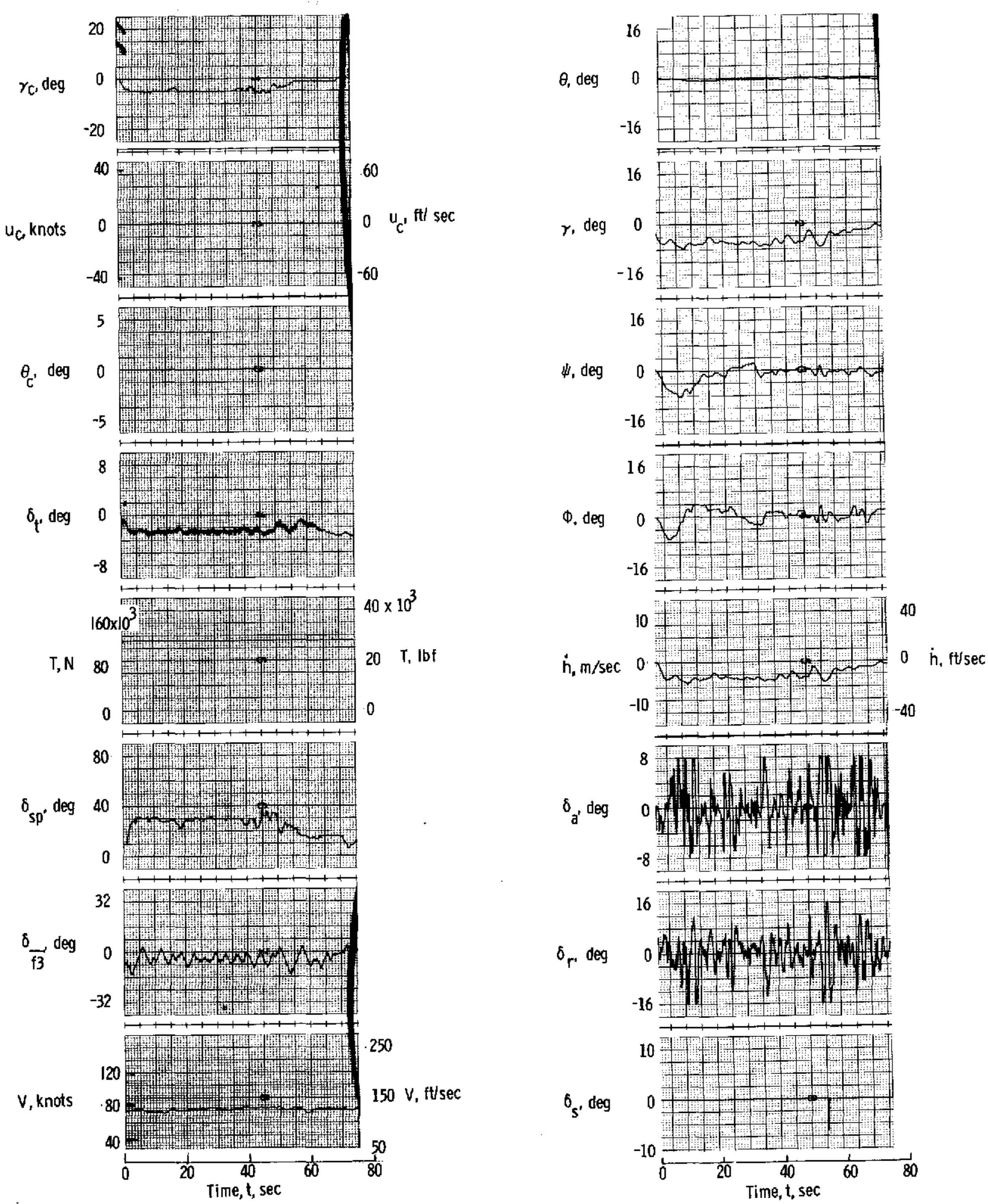


Figure 7.- Constant-speed approach using horizontal tail, flaps, and symmetric spoilers to provide decoupled longitudinal control in turbulence with $\sigma_w = 0.61$ m/sec (2 ft/sec).

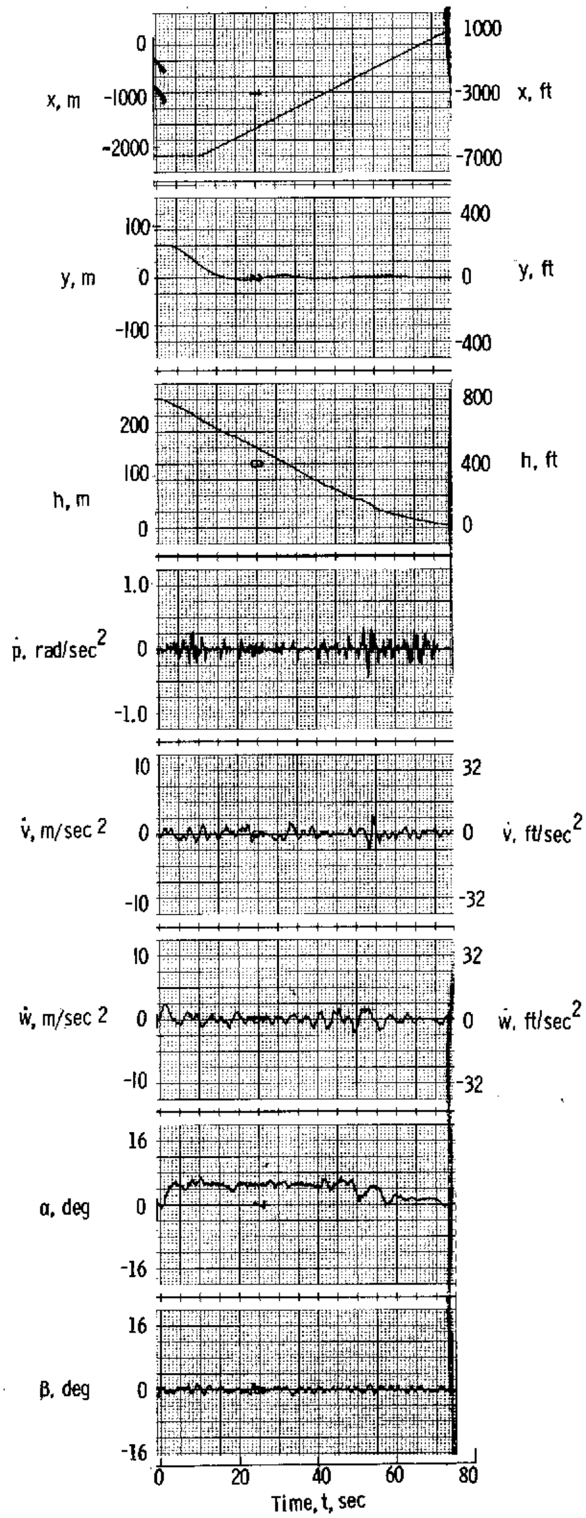


Figure 7.- Concluded.

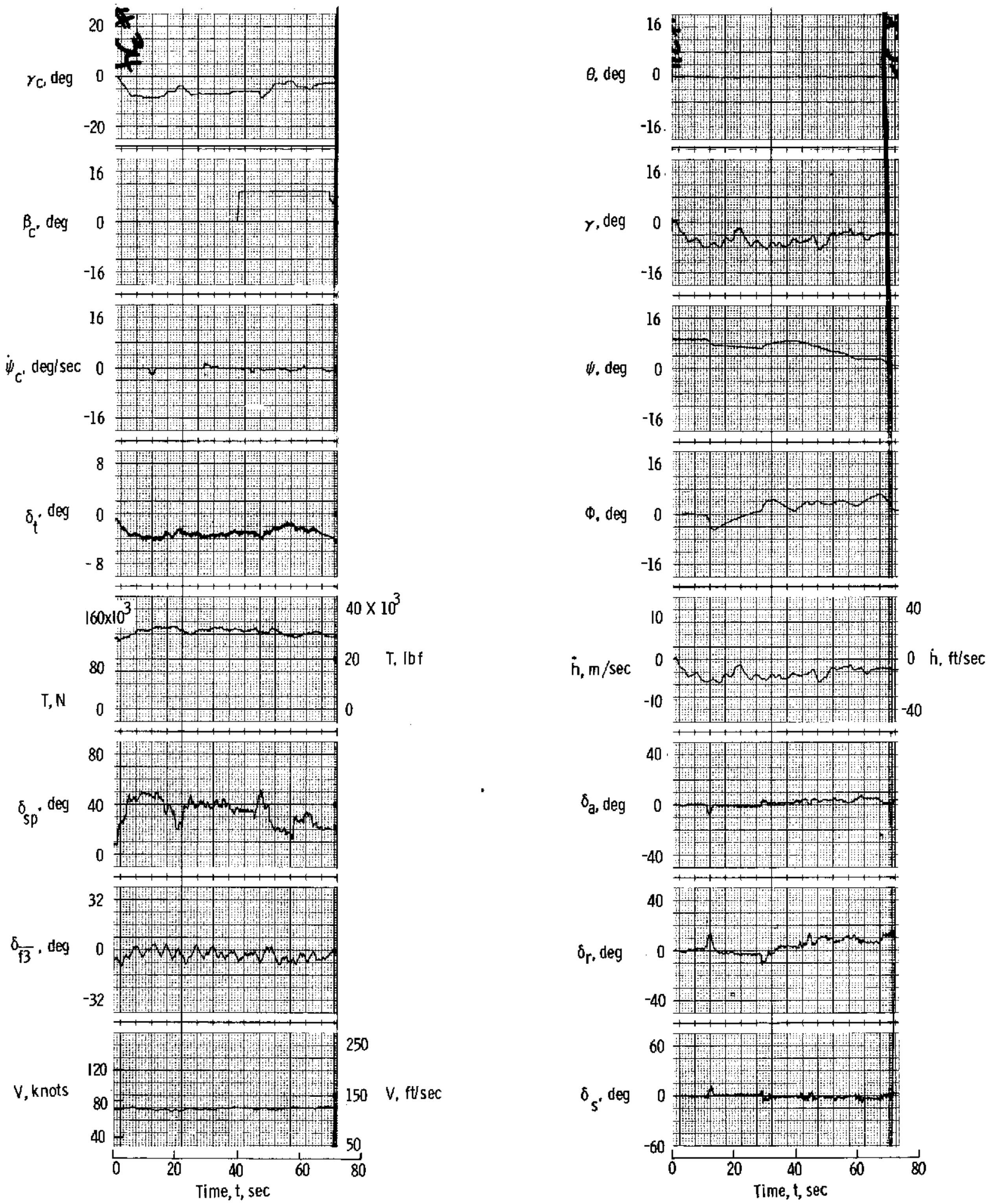


Figure 8.- Constant-speed approach using decoupled longitudinal and lateral controls in turbulence with $\sigma_w = 0.61$ m/sec (2 ft/sec).

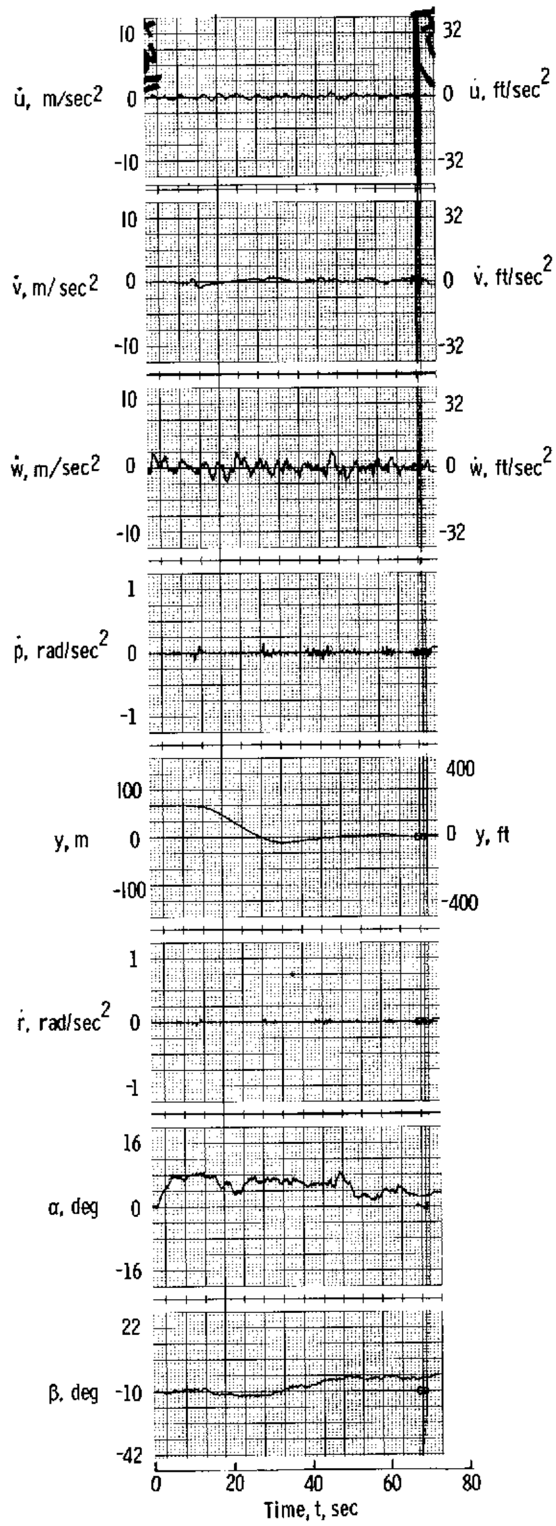


Figure 8.- Concluded.

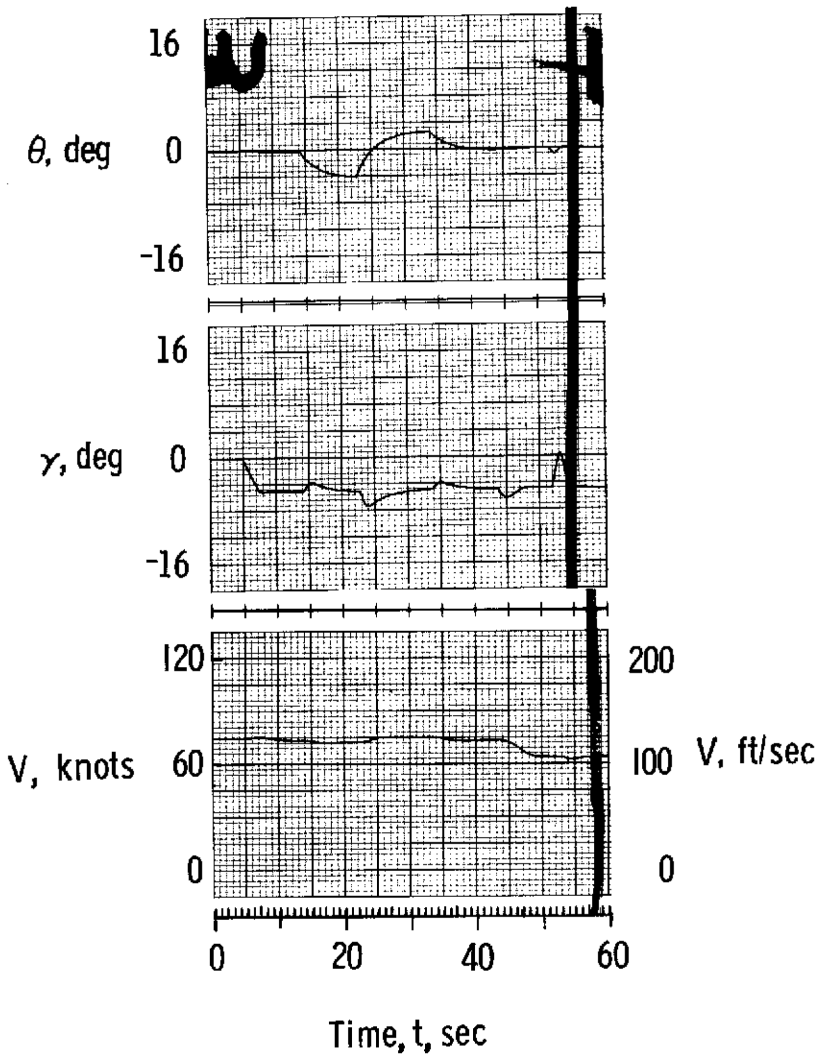


Figure 9.- Characteristics of decoupled longitudinal controls that use throttle, horizontal tail, flaps, and symmetric spoilers.

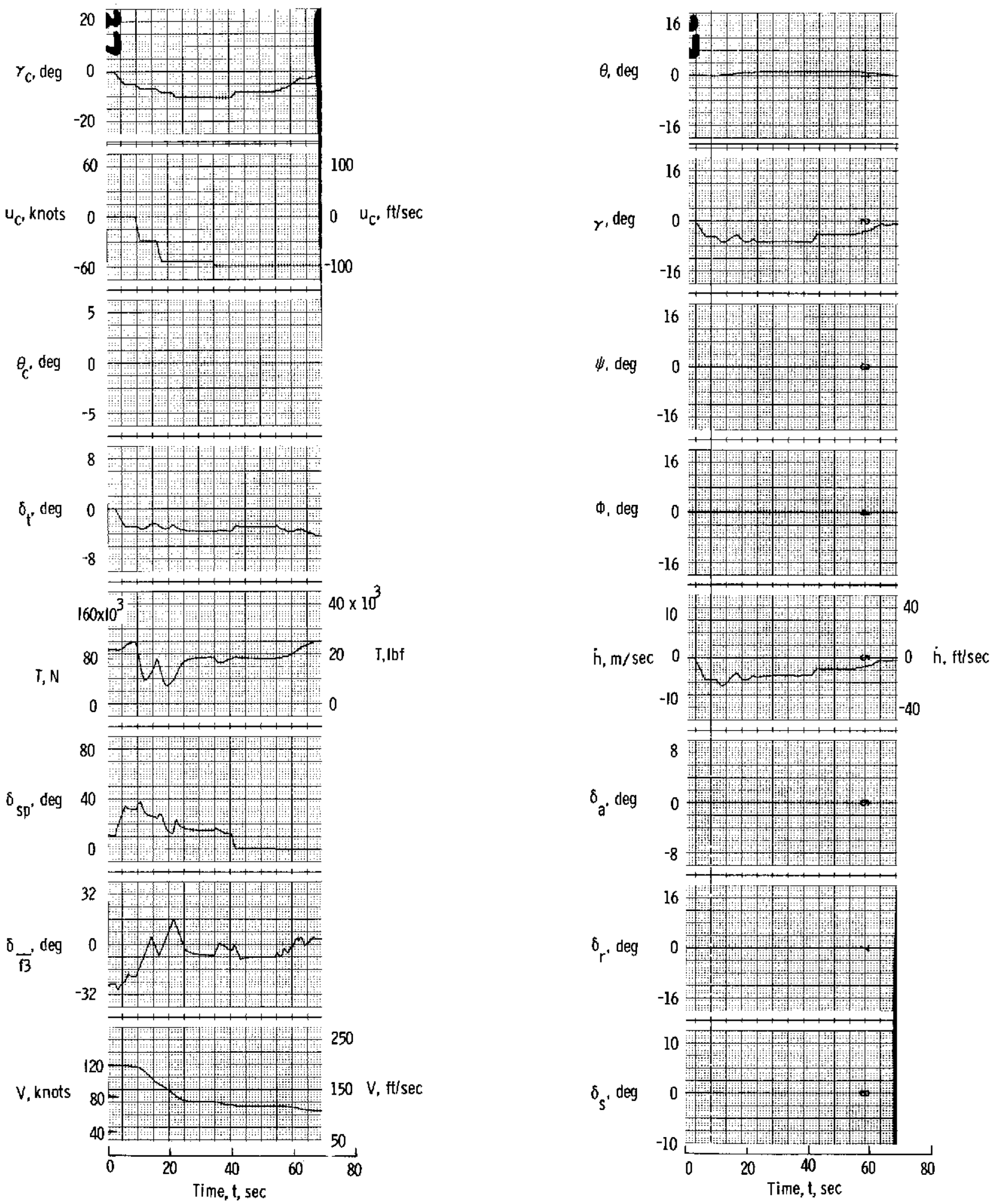


Figure 10.- Decelerating approach using throttle, horizontal tail, flaps, and symmetric spoilers to provide decoupled longitudinal and lateral control in zero turbulence.

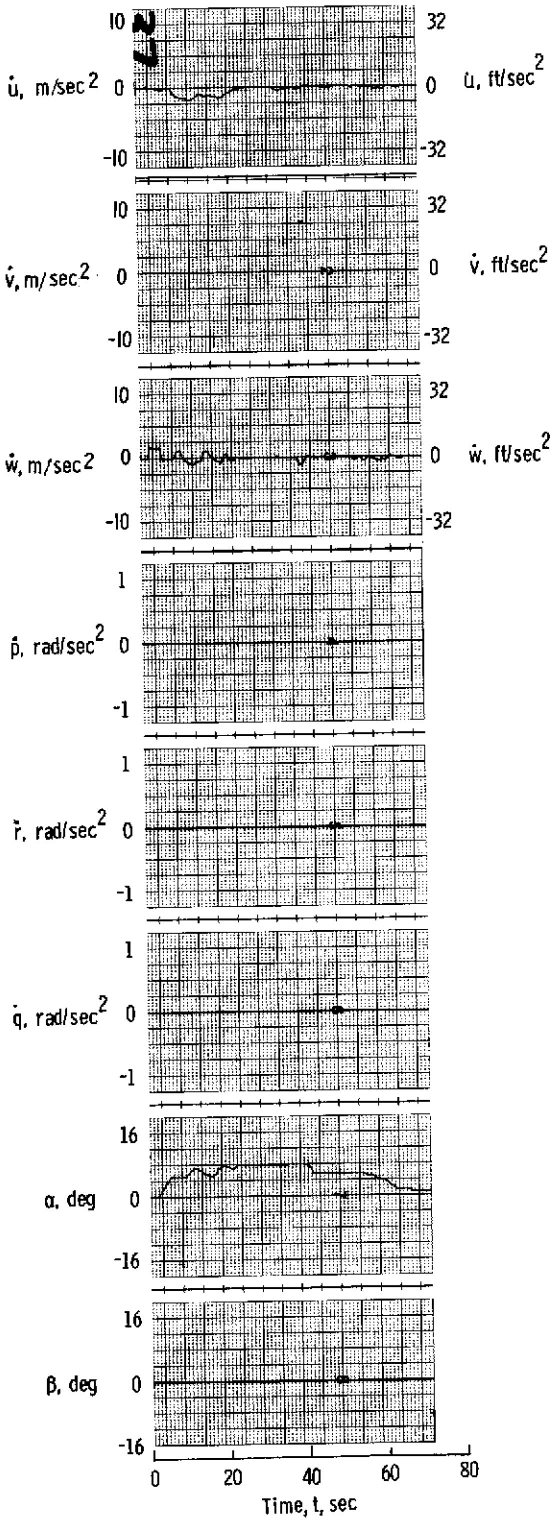


Figure 10.- Concluded.

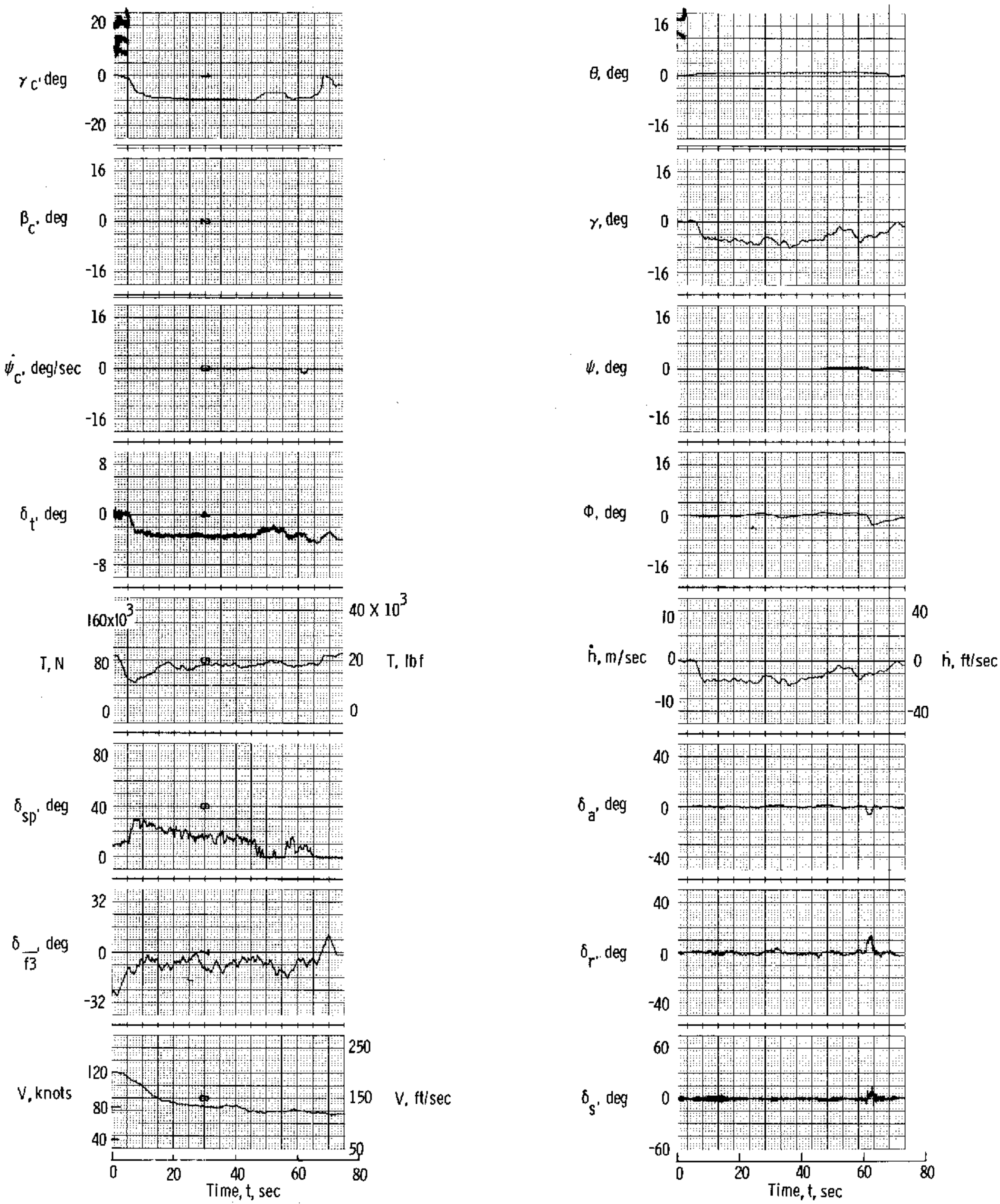


**Figure 11.- Decelerating approach using decoupled longitudinal and lateral controls with $\sigma_w$ = 0.61 m/sec (2 ft/sec).**

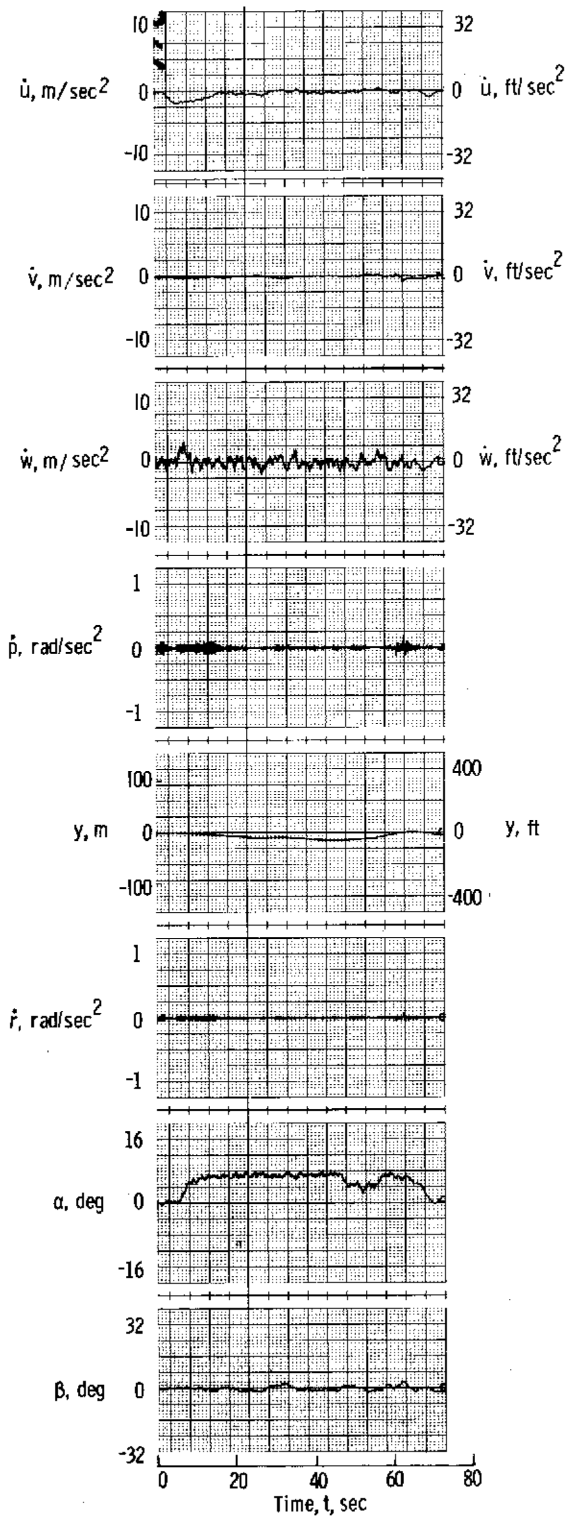


Figure 11.- Concluded.

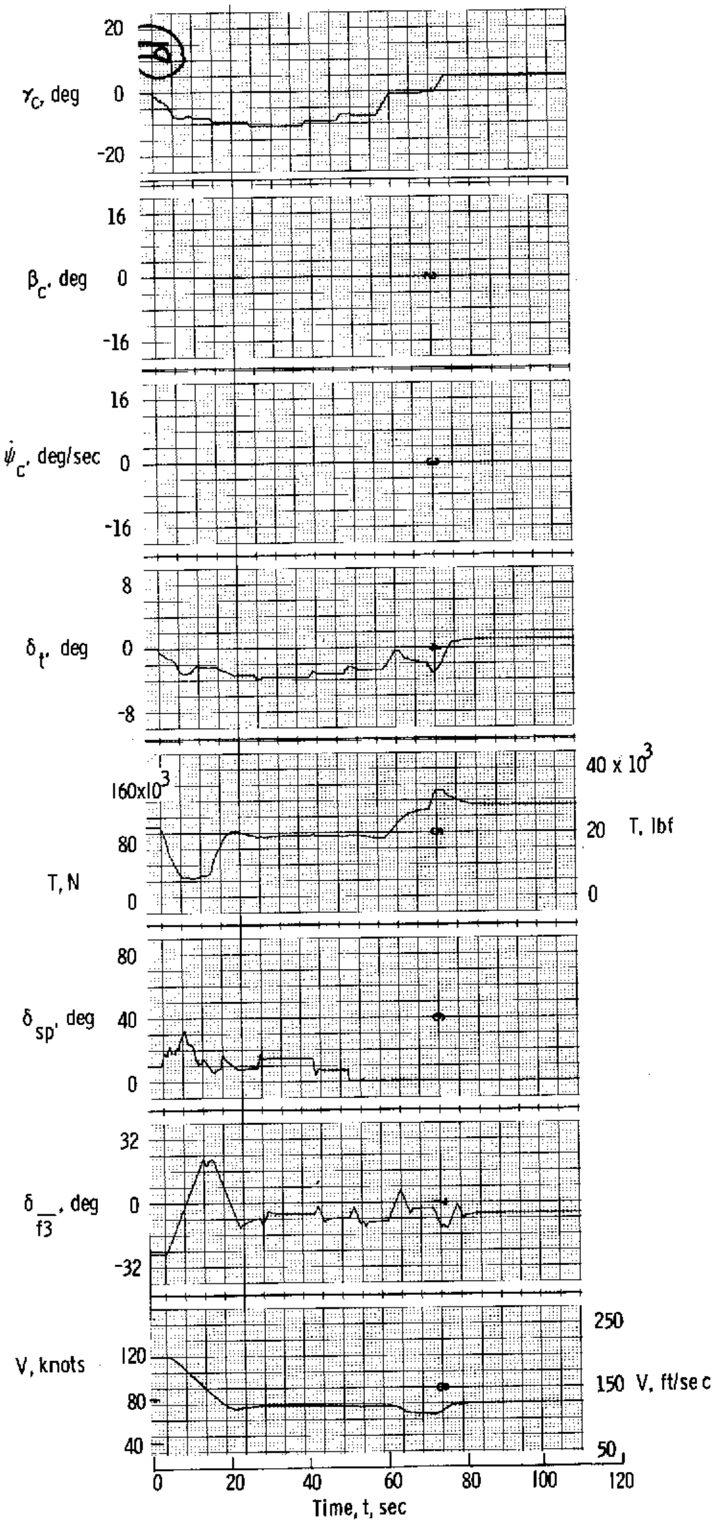


Figure 12.- Flight using decoupled longitudinal and lateral controls during a constant-speed wave-off.

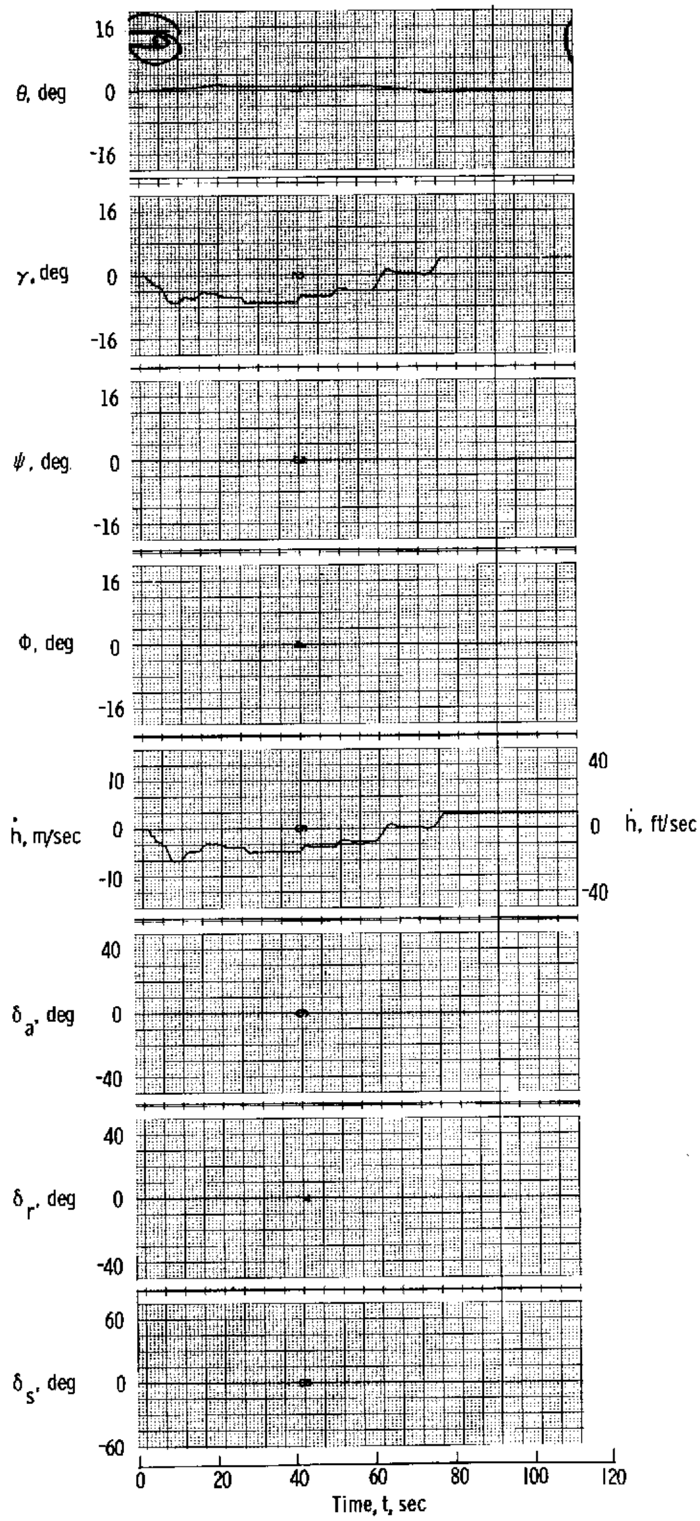


Figure 12.- Continued.

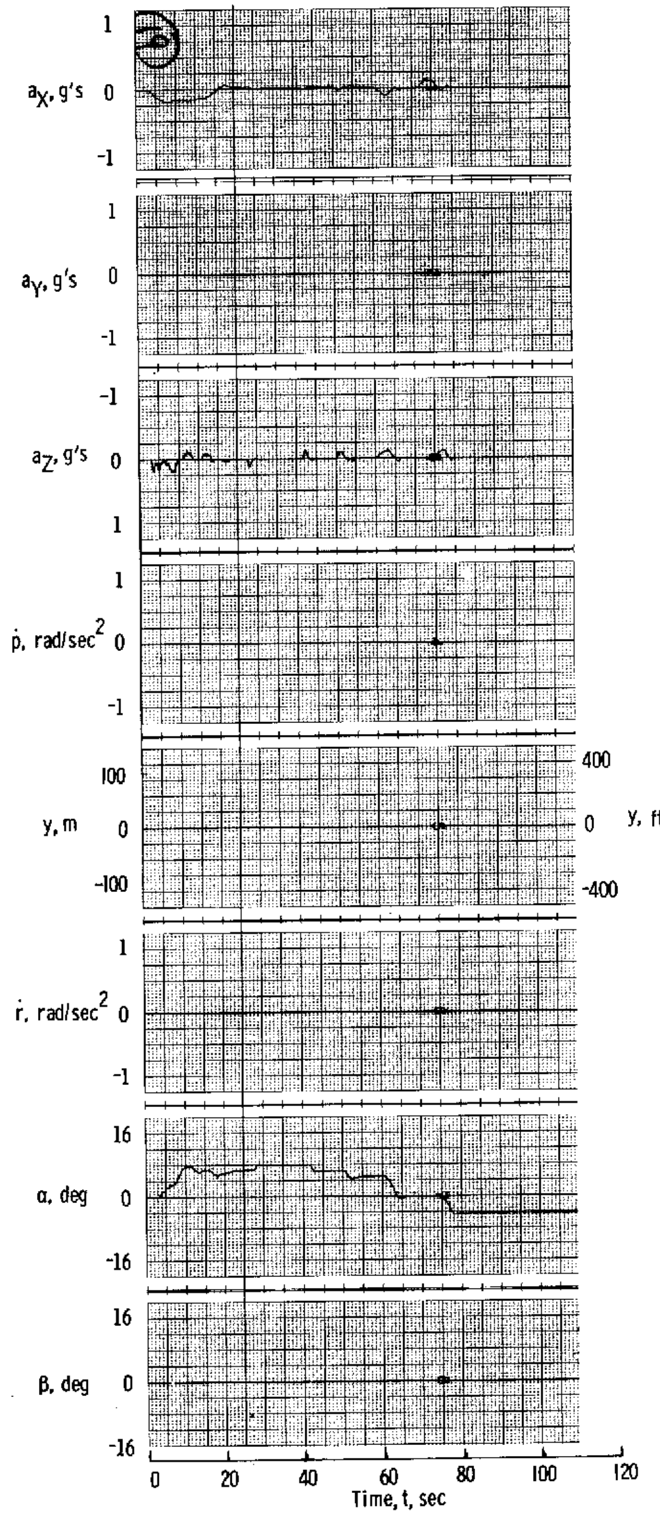


Figure 12.- Concluded.



NASA-Langley, 1974 L-8825

CAT. – 01